Nuclear Physics Mid Term Plan in Italy

LNF – Session

Frascati, December 1st - 2nd 2022

Facilities @LNS and @LNF

Magnetically-confined and laser-induced plasmas

Dario Lattuada

KORE University, Enna, Italy

Laboratori Nazionali del Sud – INFN, Catania, Italy

Istituto Nazionale di Fisica Nucleare

In-plasma nuclear reaction studies: PANDORA

Plasmas for
Astrophysics
Nuclear
Decay
Observation and
Radiation for
Archaeometry

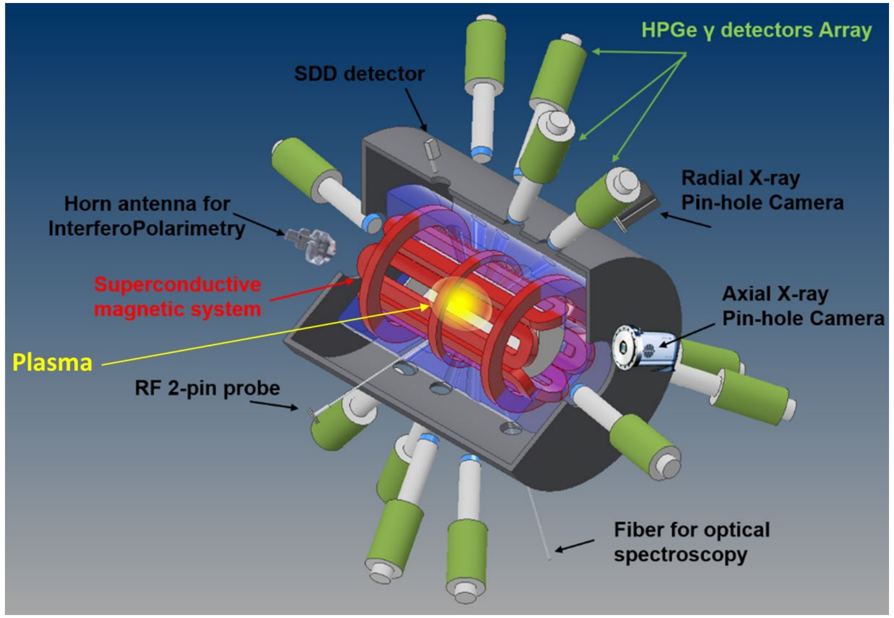

Laser-induced nuclear reaction studies: *Versatile Array for* Laser-*induced* Astrophysics Research

LOGO not available.
Fundings needed.

INSERT COIN(S)

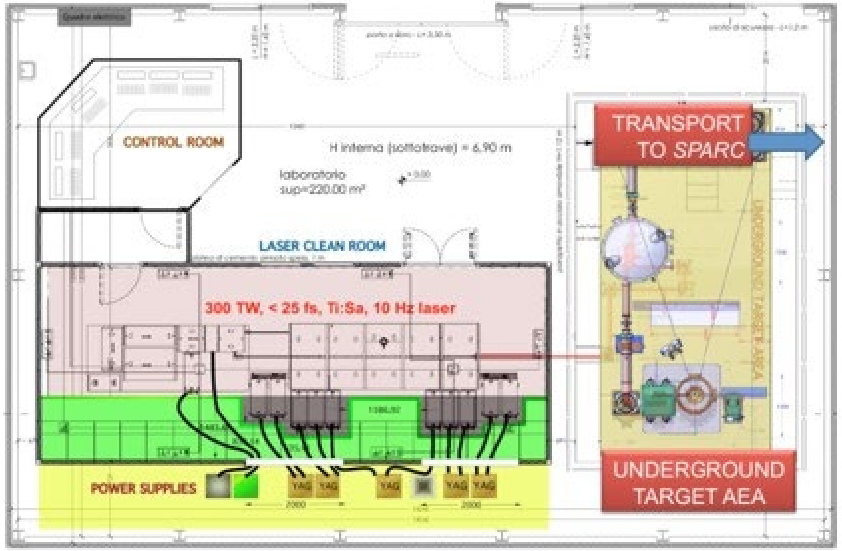

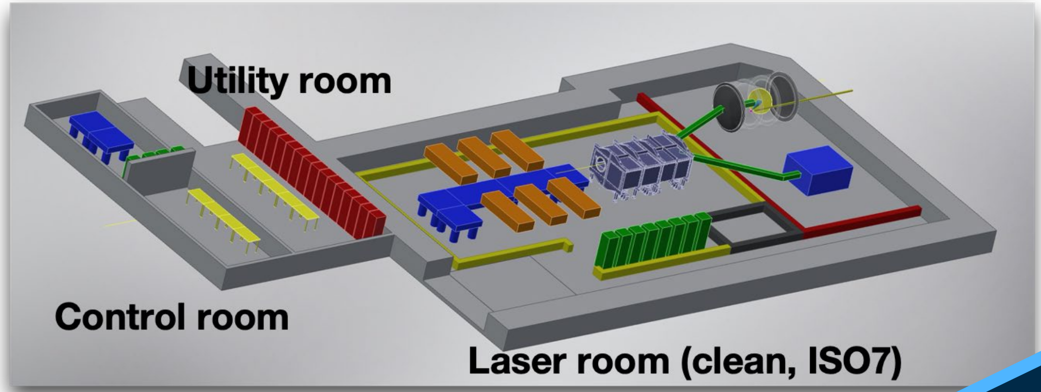

Plasmas for
Astrophysics
Nuclear
Decay
Observation and
Radiation for
Archaeometry

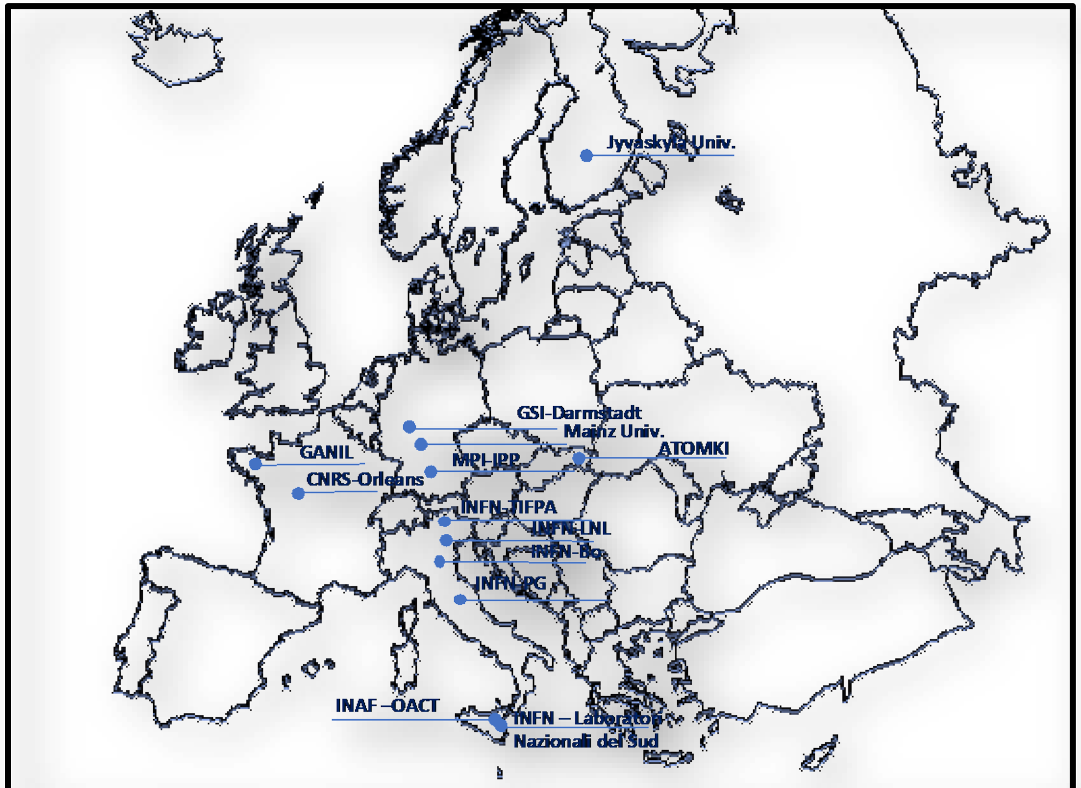

[1] INFN – Laboratori Nazionali del Sud, I-95125 Catania, Italy
[2] INFN – Sez. di Perugia, I-06123 Perugia, Italy
[3] INFN – Sez. di Bologna, I-40127 Bologna, Italy
[4] INFN – TIFPA, I- 38123 Povo TN, Italy
[5] INFN – Laboratori Nazionali di Legnaro, I-35020 Legnaro PD, Italy
[6] Department of Physics, University of Perugia, I-06123 Perugia, Italy
[7] INAF – Istituto Nazionale di Astrofisica – Osservatorio Astrofisico di Catania, I-95123 Catania, Italy
[8] Institute of Nuclear Science, ATOMKI, HU-4026 Debrecen, Hungary
[9] Max Planck Institute – Institute of Plasma Physics, D-85748, Garching
[10] INAF – Osservatorio Astrofisico d'Abruzzo, I-64100 Teramo – Italy
[11] Department of Engineering, University of Brescia, I-25123 Brescia,
[12] Department of Physics, University of Padova, I-35131 Padova, Italy
[13] Department of Electrical, Electronics and Computer Engin., University of Catania, I-95126 Catania, Italy
[14] GANIL, F-14000 Caen, France
[15] Department of Engineering, Mediterranean University of Reggio Calabria, I-89124 Reggio Calabria, Italy
[16] Department of Physics, Jyvaskyla University, FI-40014 Jyväskylä, Finland
[17] Johannes Gutenberg University Mainz, D-55122 Mainz, Germany
[18] Department of Physics, University of Milano, I-20133 Milano, Italy
[19] INFN- Sez. di Milano, I-20133 Milano, Italy
[20] Politecnico di Milano, I-20133 Milano, Italy
[21] GSI – D- 64291 Darmstadt, Germany
[22] Department of Physics, University di Camerino, I-62032 Camerino MC, Italy
[23] Agenzia Nazionale per le Nuove Tecnologie (ENEA), I-40129 Bologna, Italy
[24] Department of Physics, University of Catania, I-95125 Catania, Italy
[25] INFN – Sez. dell'Aquila, I-67100 L'Aquila,
[26] Department of Physics, Università di Trento, 38123 Povo TN, Italy
[27] CNAO, I-27100 Pavia, Italy
[28] Department of Engineering and Architecture, Università di Parma, Modena e Reggio Emilia, Italy
[29] Department of Physics, University di Messina, I-98122 Messina, Italy
[30] Department of Engineering and Architecture, Universitá degli Studi di Enna "Kore", I-94100 Enna, Italy
[31] Università degli Studi di Modena e Reggio Emilia Dipartimento di Ingegneria Enzo Ferrari: Modena, IT

PANDORA is a facility whose construction is supported by INFN in the frame of PANDORA_Gr3 project; it aims at building an innovative compact and flexible magnetic plasma trap, for fundamental physics studies and interdisciplinary and applied research. The main goal is the study of β-decays in the plasma (never done so far), i.e. in ionization conditions similar to some stellar environments and relevant for nucleosynthesis of chemical elements in the cosmos.

Takahashi et al. 1987, Phys Rev C 36, 1522

Plasmas for
Astrophysics
Nuclear
Decay
Observation and
Radiation for
Archaeometry

1) **for the first time, β-decay measurements** in plasmas; → **Huge impact on nuclear physics and stellar nucleosynthesis**

2) **plasma opacity measurements in conditions similar to kilonovae ejecta**; → **Heavy elements production in n-star merging**

3) **an unprecedented setup for applications**: it will be the biggest B-minimum magnetic trap with potentiality as ion source; as testbench for magnetic fusion; as radiation source for Archeometry. → **New ion and radiation sources for science and technology**

A NEW CHALLENGE: Reproduce in laboratory some stellar-like conditions and measure the expected variations of nuclear lifetime in β–decaying nuclei

PANDORA:
- **Magnetic Trap**
- **Plasma Diagnostics System**
- **HPGe γ-detectors Array**

D. Mascali et al., *Universe* **2022**, 8(2)

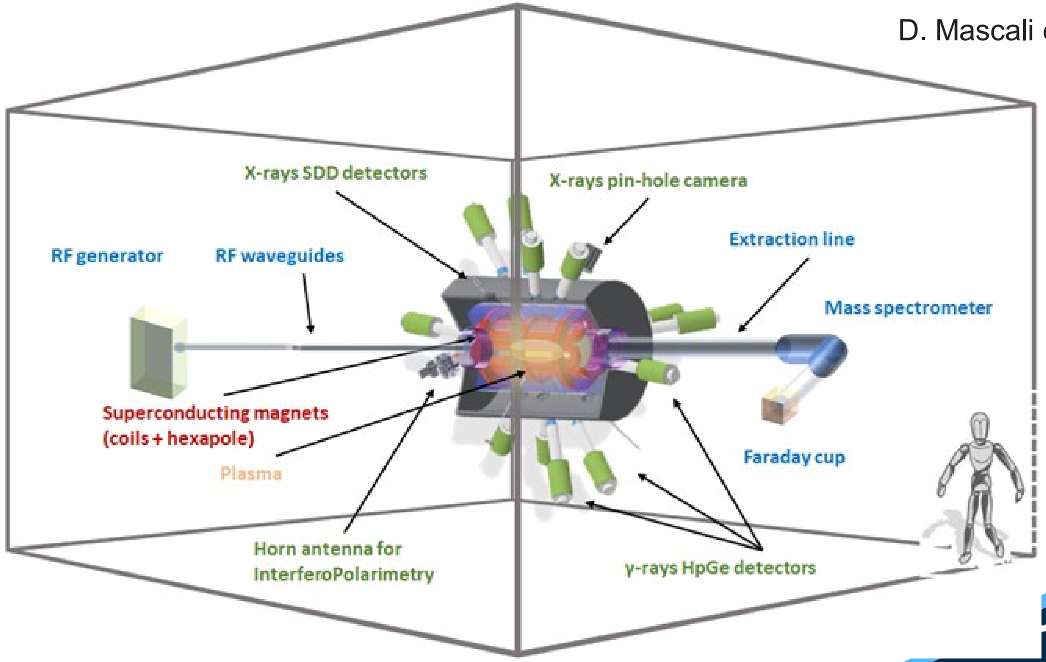

1. An innovative superconducting **magnetic plasma trap**, able to produce and confine plasmas with electron-ion density up to 10^{13} cm^{-3} and electron temperature of T_e~0.1-30 keV;
2. An advanced **plasma multi-diagnostic system**, consisting in a set of non-invasive diagnostic tools capable of operating simultaneously for the non-intrusive monitoring of the plasma thermodynamic properties and the measurement of plasma parameters;
3. An **Array of 14 HPGe (High-purity Germanium) detectors** for γ-ray spectroscopy, surrounding the plasma trap.

Goal: to investigate Electron-Cyclotron-Resonance plasma thermodynamical proprieties (electron density and temperature) in compact trap;

→ A gas or a metallic material vaporized by an oven is fluxed inside a plasma chamber

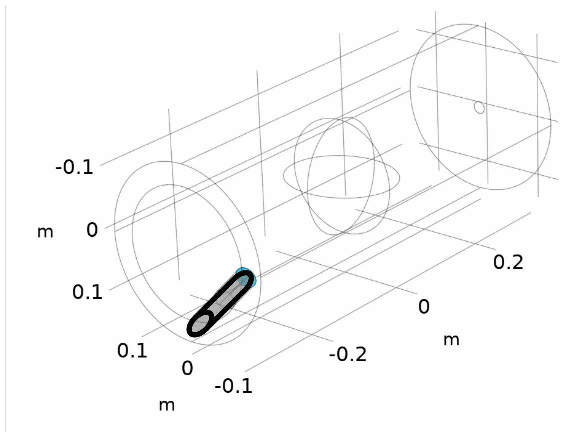

→ Plasma is excited by Electron-Cyctron-Resonance by microwaves and confined by magnetic fields

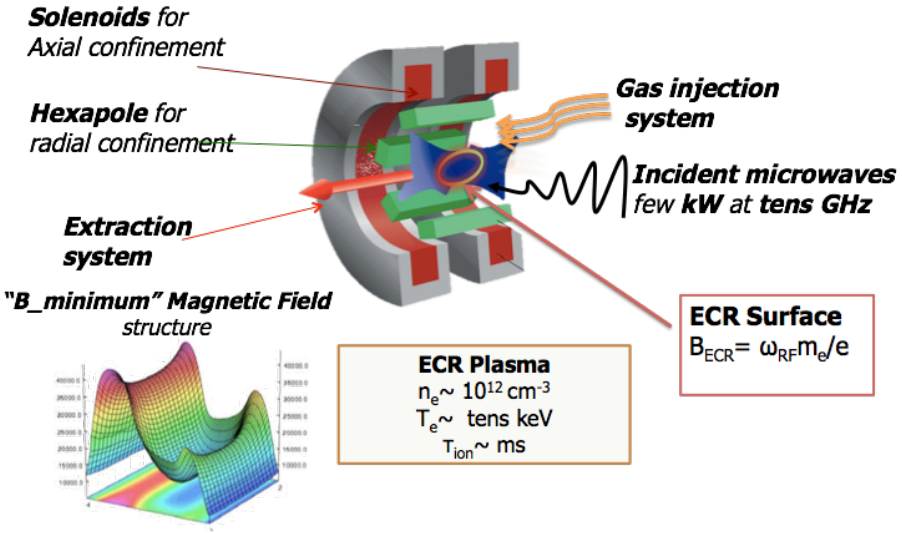

→ A multidiagnostic system surrounding the plasma chamber was developed to measure plasma parameters

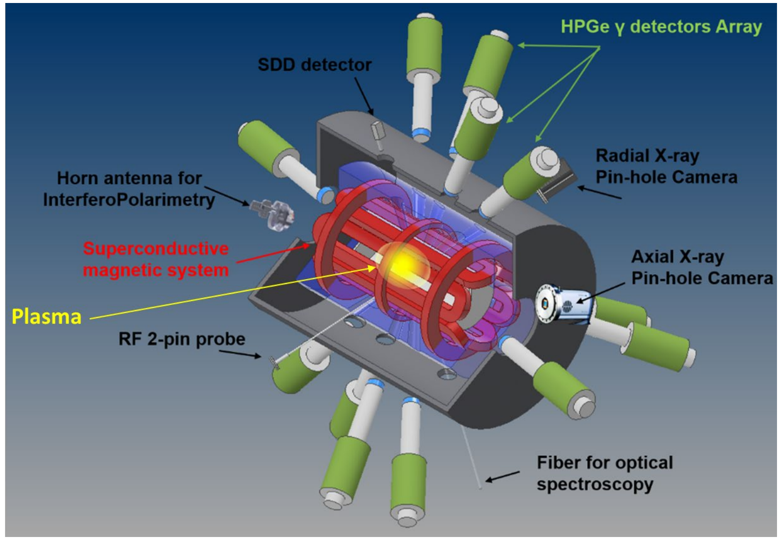

Method: ECR plasmas emit radiation from microwave to hard X-rays and this radiation can be used to investigate plasma parameters in different regimes;

Plasma Emitted Radiation

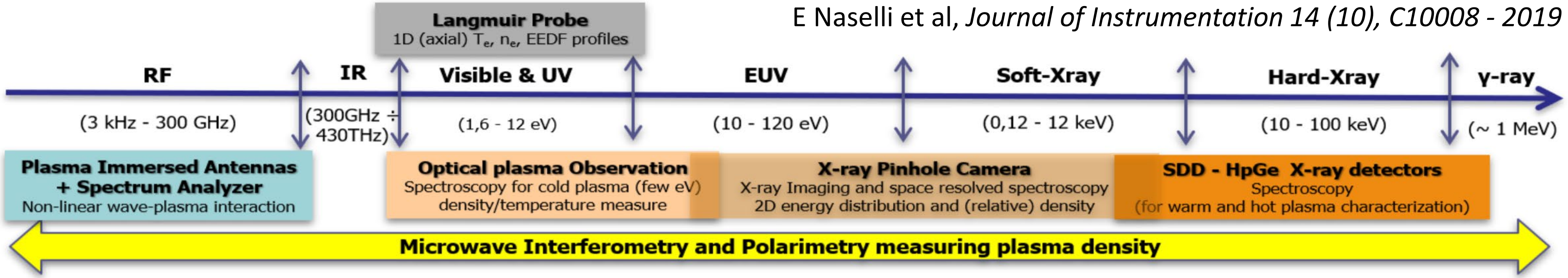

E Naselli et al, *Journal of Instrumentation 14 (10), C10008 - 2019*

PANDORA: 14 HPGe detector array surrounding the plasma trap

GS Mauro et al, Frontiers in Physics, 621(2022)
E Naselli et al, *Frontiers in Physics, 692 (2022)*
A Gausdouff et al, *Frontiers in Physics, 2022*

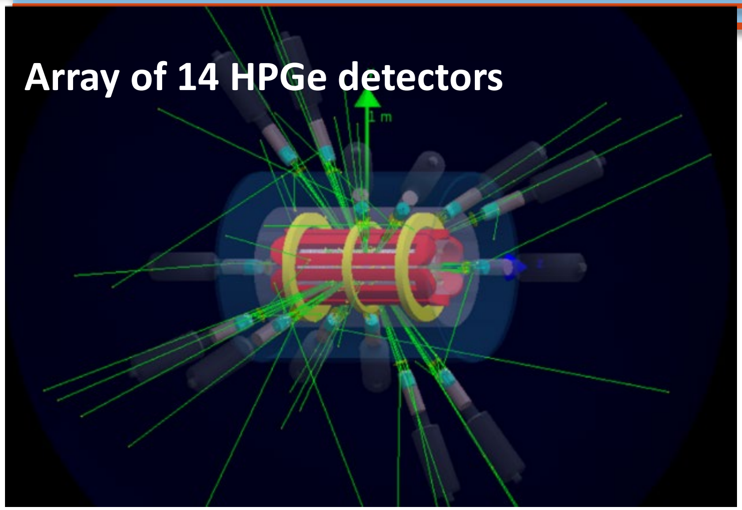

PANDORA: Online plasma multidiagnostic

E Naselli et al, *Journal of Instrumentation 14 (10), C10008 - 2019*

Diagnostic tool	Sensitive Range	Measurement	Resolution - Measure Error
SDD	1 ÷ 30 keV	Volumetric soft X-ray Spectroscopy: warm electrons temperature and density	Resolution ~ 120 eV ε_{ne} ~ 7%, ε_{Te} ~ 5%
HPGe detector	30 ÷ 2000 keV	Volumetric hard X-ray Spectroscopy: hot electrons temperature and density	FWHM @ 1332.5 keV < 2.4 keV ε_{ne} ~ 7%, ε_{Te} ~ 5%
Visible Light Camera	1 ÷ 12 eV	Optical Emission Spectroscopy: cold electrons temperature and density	$\Delta\lambda$ = 0.035 nm R = 13900
X-ray pin-hole camera	2 ÷ 15 keV	2D Space-resolved spectroscopy: soft X-ray Imaging and plasma structure	Energy Resolution ~ 0.3 keV Spatial Resolution ~ 0.5 mm
W-band super-heterodyne polarimeter	W-band 90 ÷ 100 GHz	Plasma-induced Faraday rotation: line-integrated electron density	ε_{ne} ~ 25%
Microwave Imaging Profilometry (MIP)	60 ÷ 100 GHz	Electron density profile	ε_{ne} ~ 1% ÷ 13%
Multi-pins RF probe	10 ÷ 26.5 GHz	Local EM field intensity	ε ~ 0.073 ÷ 0.138 dB
Multi-pins RF probe + Spectrum Analyzer (SA)	10 ÷ 26.5 GHz *(probe range)*	Frequency-domain RF wave	SA Resolution bandwidth: RBW = 3 MHz
Multi-pins RF probe + Scope + HPGe detector	10 ÷ 26.5 GHz *(probe range)*	Time-resolved radiofrequency burst and X-ray time-resolved Spectroscopy	80 Gs/s *(scope)* time scales below ns
Thomson Scattering	0.5 ÷ 500 eV	EEDF, absolute electron density global electron drift velocity	Condition-dependent (a function of spectral width, dependent on temperature, and area, dependent on density)

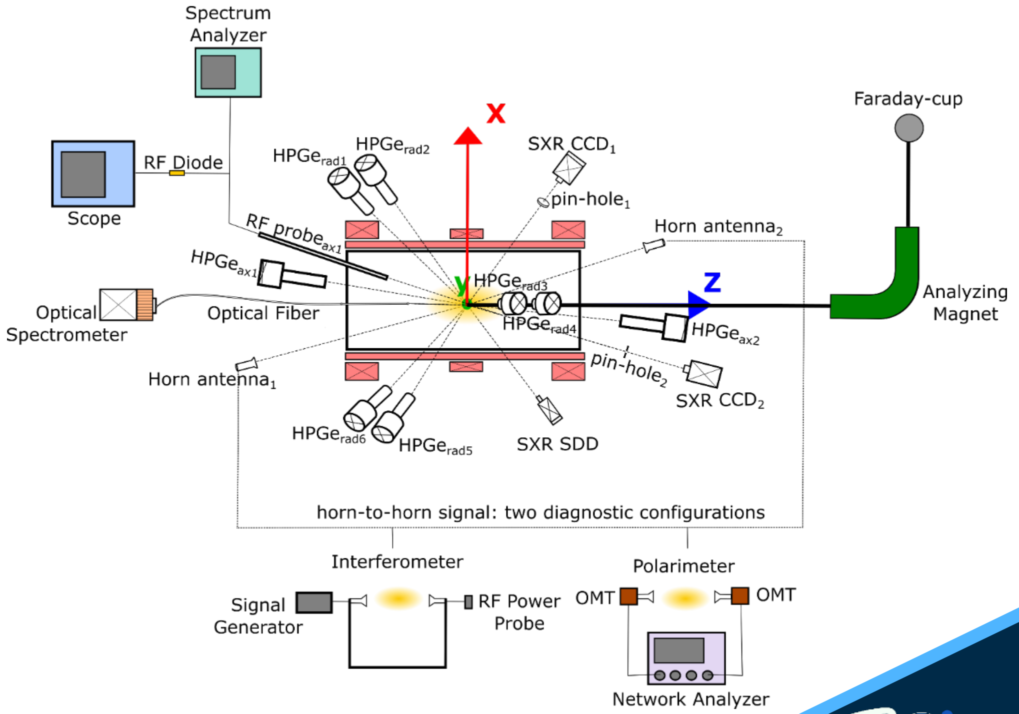

Microwave Polarimetry for the non-invasive measurement of the plasma density

Polarimetric system based on 2 horn-antennas coupled with 2 OMTs (one of which is rotating) operating at 18-26.5 GHz

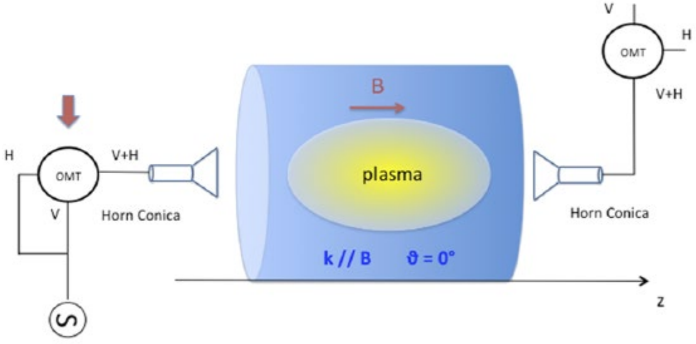

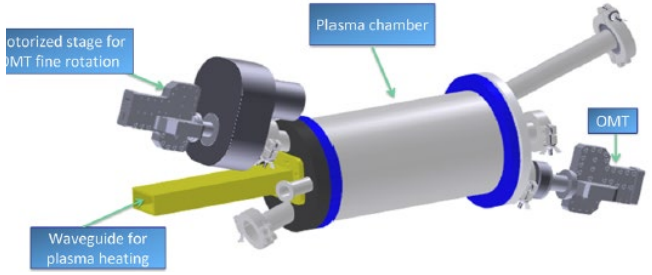

$$\vartheta_F = \frac{\omega}{c}\frac{1}{2}\left(\sqrt{1-\frac{\omega_p^2}{\omega(\omega-\omega_g)}}-\sqrt{1-\frac{\omega_p^2}{\omega(\omega+\omega_g)}}\right)$$

Polarimetry: density measurement is based on the evaluation of the Faraday rotation angle of the polarization plane of an e.m. wave that passes through the magnetoplasma

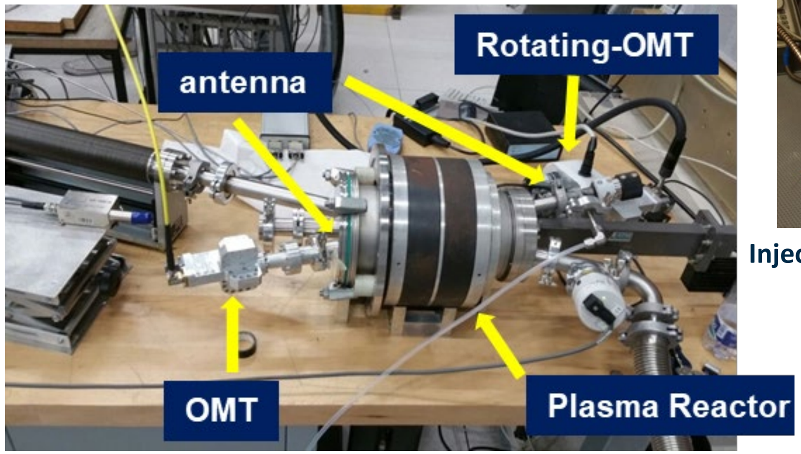

OrthoMode Transducer (OMT)

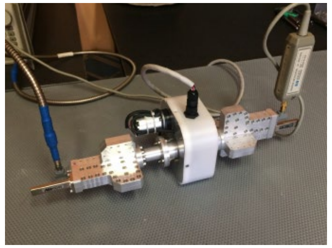

Horn antennas

Injection and extraction flanges with horn-antennas

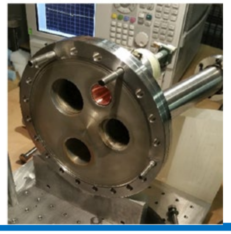

Polarimetry: based on the evaluation of the Faraday rotation angle of the polarization plane of an e.m. wave that passes through the magnetoplasma

$$\theta = \int_0^L \frac{\omega}{2c}\left[\sqrt{1-\frac{\omega_p^2}{\omega(\omega-\omega_{ce})}}-\sqrt{1-\frac{\omega_p^2}{\omega(\omega+\omega_{ce})}}\right]\cdot dz \sim \left(\frac{e^3}{2\pi m^2 c^4}\int_0^L n_e B\cdot dz\right)\lambda^2 = RM\ \lambda^2$$

O-wave and X-wave different propagation constant in anisotropic plasma

Known the magnetic field B, by a fitting procedure is possible to measure the plasma density:

$n_e = 2.93 \pm 0.8 \cdot 10^{18}\ m^{-3}$

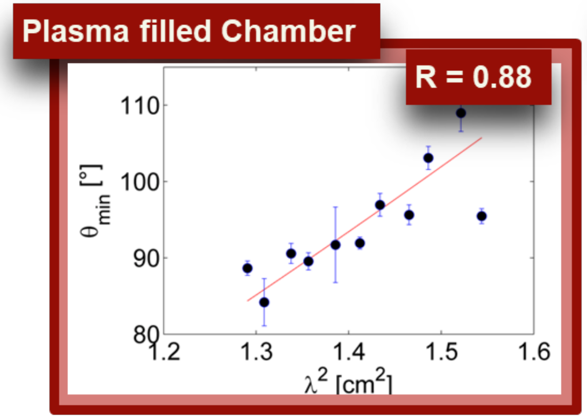

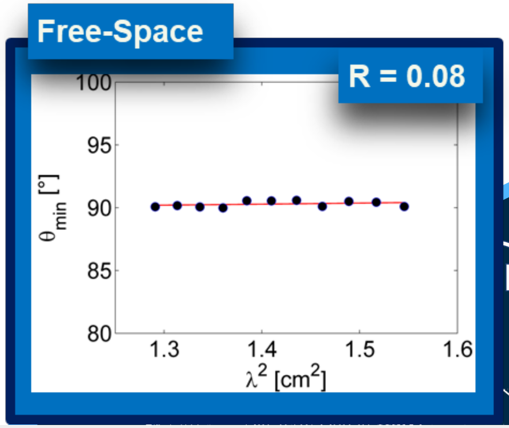

E. Naselli et al., Journal of Instrumentation, Vol13, (2018).

Experimental Testbench: OMT-based K-band scheme

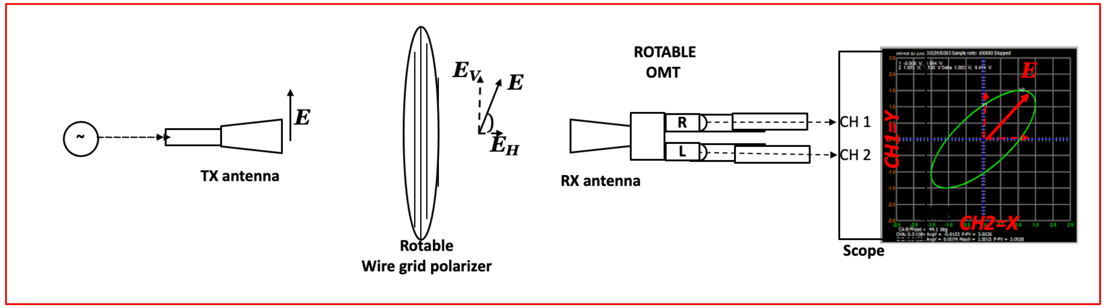

experimental arrangement

Wire-grid polarizer SETUP

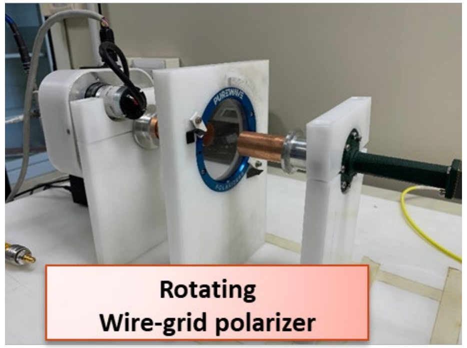

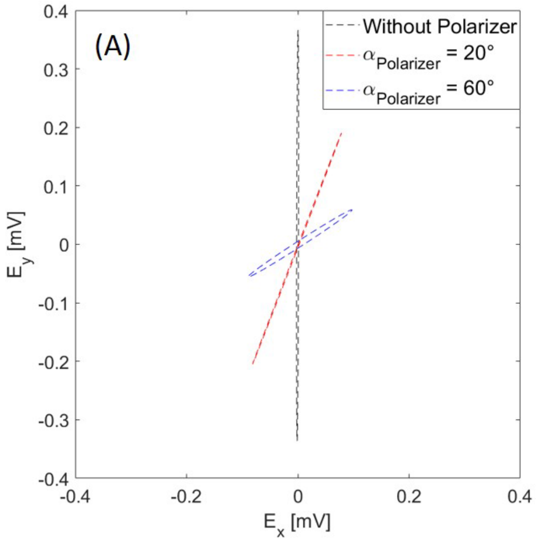

(A)

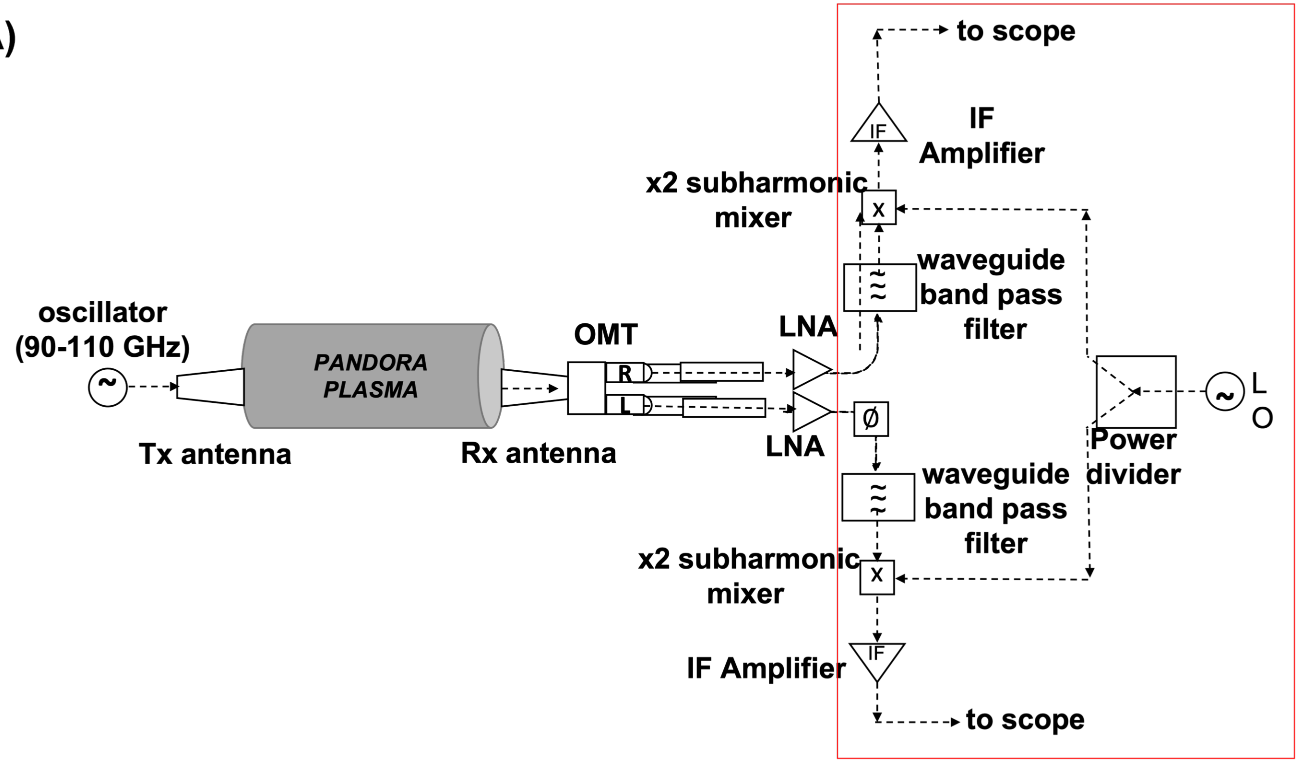

Super-heterodine scheme for Stokes Parameters detection in magnetized plasmas: simplified block-diagram of the mm-wave polarimeter for PANDORA.

G. Torrisi et al., Front Astron Space Sci (2022) 9:949920

Soft X-ray Imaging and Space-resolved spectroscopy for the local measurement of plasma density and temperature

CCD Camera

- Sensitivity range ~ 2 ÷ 20 keV
- Sensor Size: 13.3 mm x 13.3 mm (1024 x 1024 Pixels)
- Pixel size: 13 μm x 13 μm
- Lead Pin-hole (diameters 400 μm)

- **Energy Resolution ~ 260 eV @ 8 keV**
- **Spatial Resolution ~ 450 μm**

Soft X-ray pin-hole camera tool

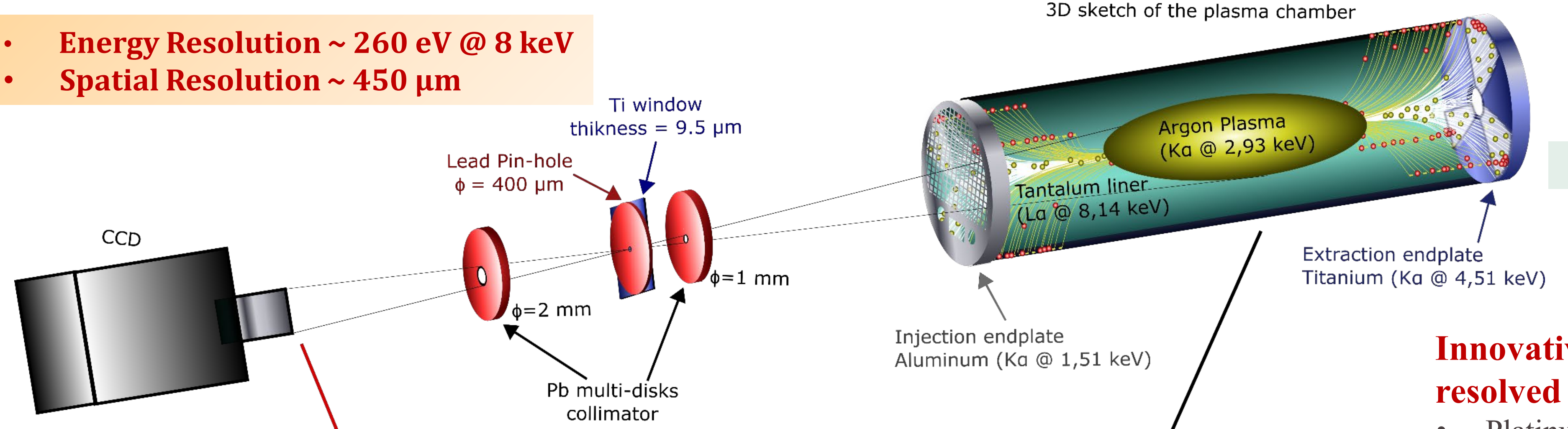

Typical X-ray image acquired by the CCD

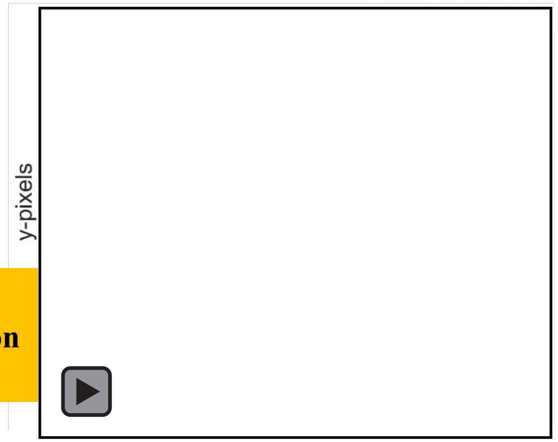

"Live" plasma structure and emission investigations

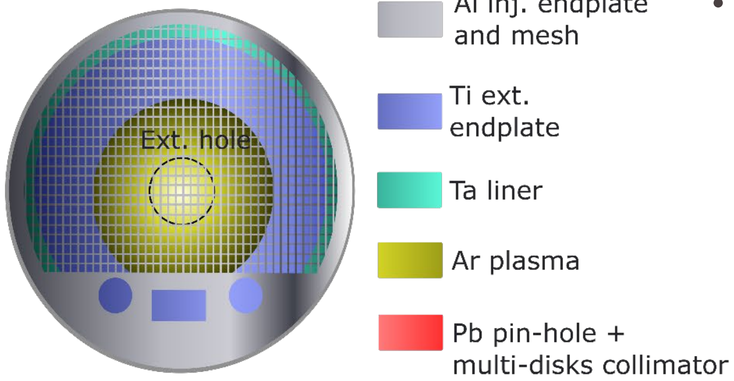

Advanced design of the plasma chamber walls

Fluorescence lines can be used to get info about where the electrons collide on the chamber walls

(plasma vs losses X-radiation emission)

Innovative soft X-ray Shutter for time resolved measurements:

- Platinum-Iridium (PtIr) material;
- 6 mm aperture diameter;
- Capable of blocking X-ray energy up to 30 keV;
- Total opening time: 4.4 milliseconds

S. Biri et al., Journal of Instrumentation 16 (2021) 02006

Advanced Algorithm for Single Photon Counted (SPhC) Analysis

Spatially-resolved X-ray Spectroscopy

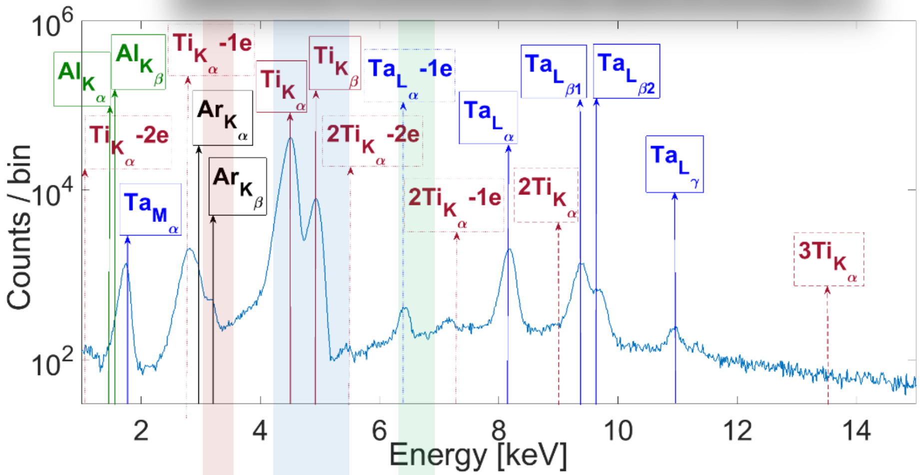

Ar **Ti** **Ta**

Plasma structure inspection

Axial losses inspection

Radial losses inspection

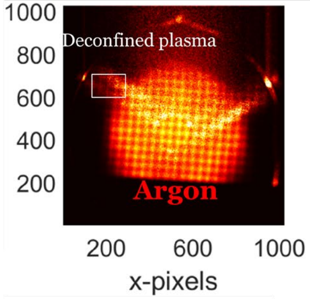

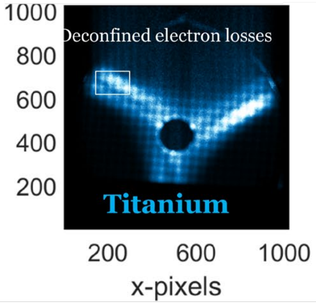

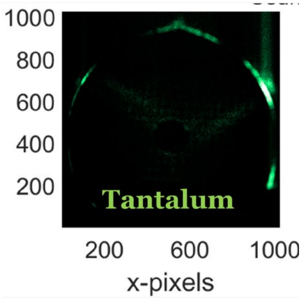

It is possible pixel-by-pixel to investigate the balance between plasma emissions vs. losses emissions

Plasma radius evaluation (uncertainty of 5%)

In SPhC each pixel becomes an independent spectrally-sensitive detector: decoupling of photon number vs. energy

POWERFUL Investigations:
SPATIALLY-RESOLVED SPECTROSCOPY

The data on the spectrum contains the spatial information on the emitting positions:

the definition of a ROI allows the imaging of the elemental distribution.

High spatial and energy resolutions:

- **Energy Resolution ~ 260 eV @ 8 keV**
- **Spatial Resolution ~ 450 µm**

Spectrally-resolved X-ray Imaging

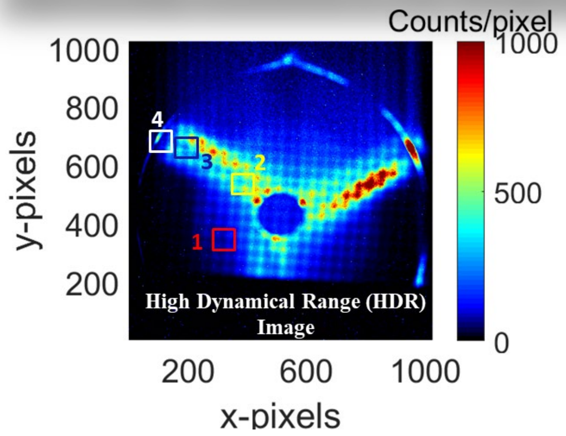

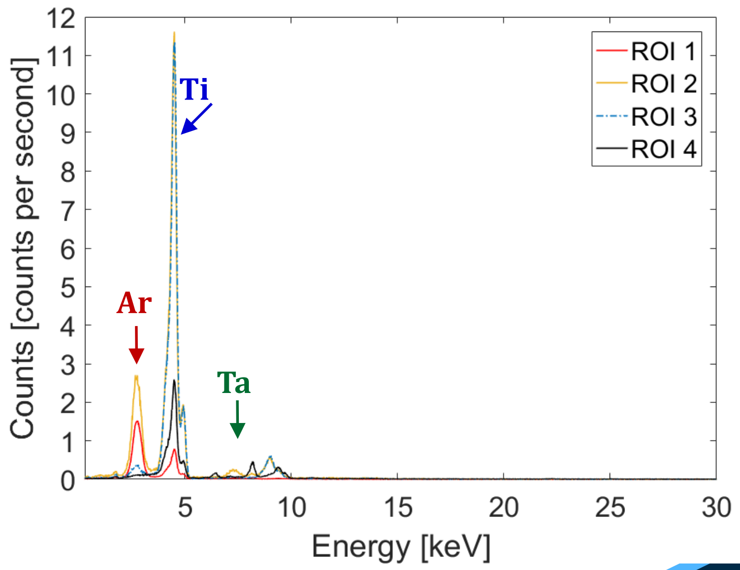

Analyzing each ROI-spectrum it is possible locally measure the plasma parameters (electron density, temperature)
Comparing experimental spectrum vs. theoretical one

E. Naselli et al., Condensed Matter 7(1), 5, 2022
E. Naselli et al., JINST (2022) **17** C01009
S. Biri et al., JINST 16, 2021, P03003

B. Mishra et al., Physics of Plasmas 28, 102509 (2021)
B. Mishra et al., Condensed Matter 6(4) (2021) 4

Towards PANDORA…

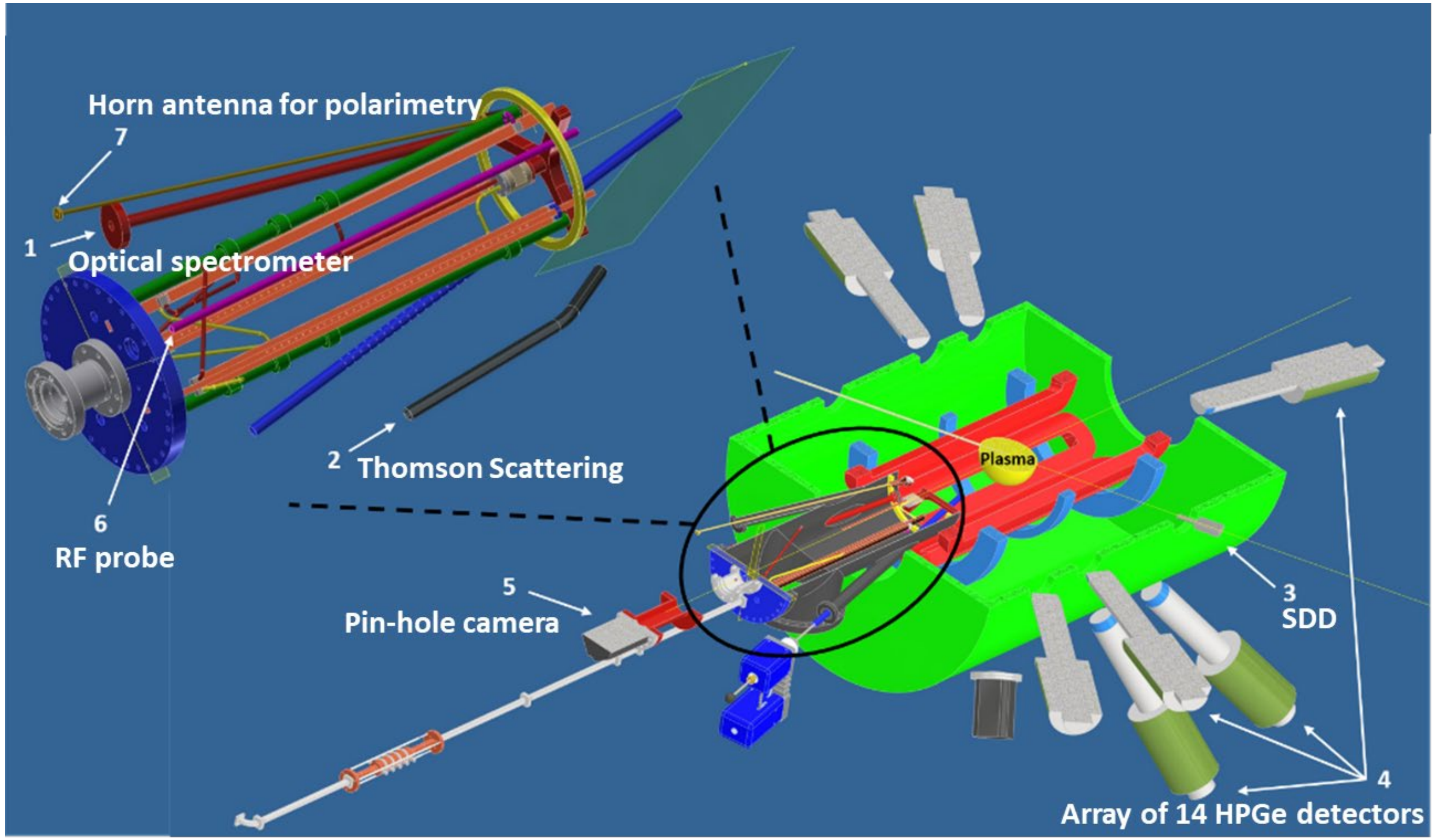

Multi-diagnostics approach in the Flexible Plasma Trap @ INFN-LNS

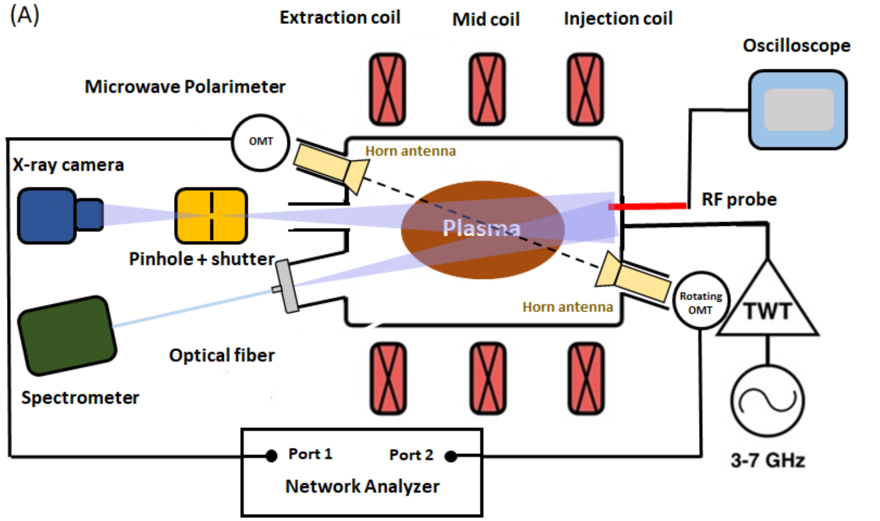

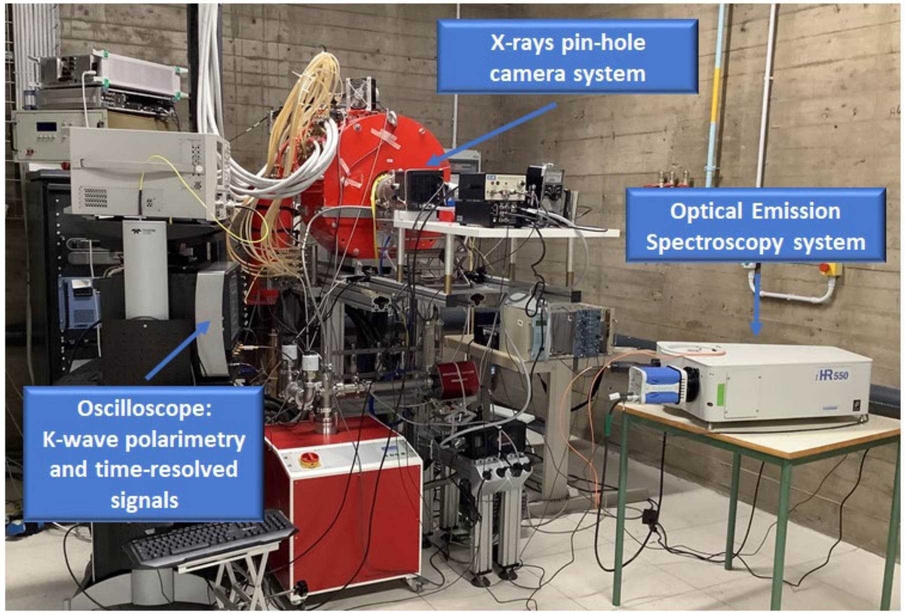

Versatile Array for Laser-induced Astrophysics Research

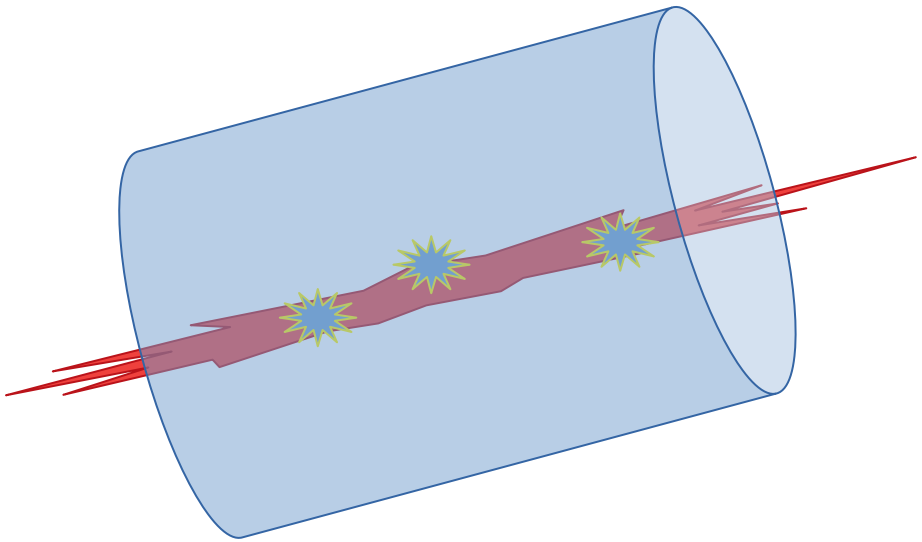

← Yes, we do need a logo

D. Lattuada, G.L. Guardo, A. Bonasera, M. La Cognata, A. Tumino, L. Lamia, A.A. Oliva, S. Palmerini, R.G. Pizzone, G.G. Rapisarda.

University of Texas – CHEDS, Austin, US
Cyclotron Institute, Texas A&M, US
ELI-NP - IFIN-HH, Bucharest, Romania
ENEA ABC, Frascati, Italy

Curtesy of A. Tumino

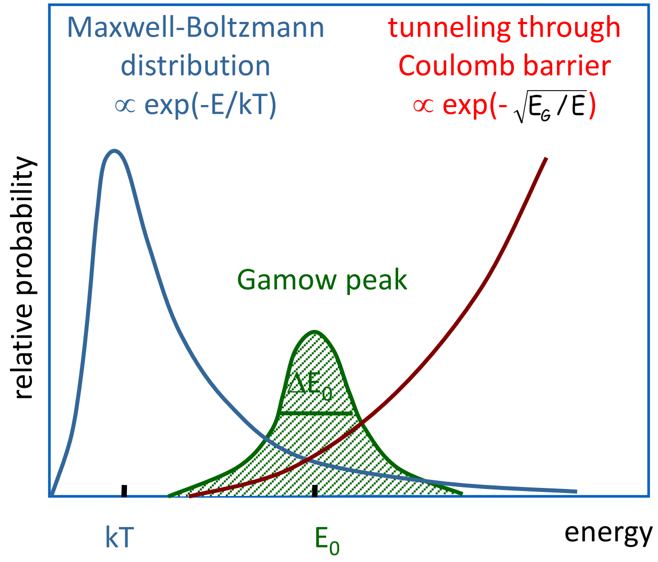

Example: T ~ 15x10^6 K (T_6 = 15)

reaction	C.barrier (MeV)	E_0 (keV)	area under Gamow peak
p + p	0.5	5.9	7.0x10^{-6}
α + ^{12}C	2.242	56	5.9x10^{-56}
^{16}O + ^{16}O	10.349	237	2.5x10^{-237}

For T ~ 200x10^6 K, E_0 ~ 320 keV
KT ~ 17 keV

Gamow peak: most effective energy region for thermonuclear reactions

It is where measurements should be carried out

10^{-18} barn < σ < 10^{-9} barn ➡

- EXTRAPOLATION
- LUNA MV – JUNA: with background suppression

.. explore directly in laboratory plasmas!

Evaluating the electron screening

Relatively small enhancements due to electron screening at energies E/U = 100 could cause significant errors in the extrapolation to lower energies, if the cross-section curve is forced to follow the trend of the enhanced cross sections without correcting for screening.

The whole effect of screening in this case ($U_0 << E_{max}$) *is then that the reaction rate with screening neglected has to be multiplied by the factor* $e^{-\frac{U_0}{KT}}$

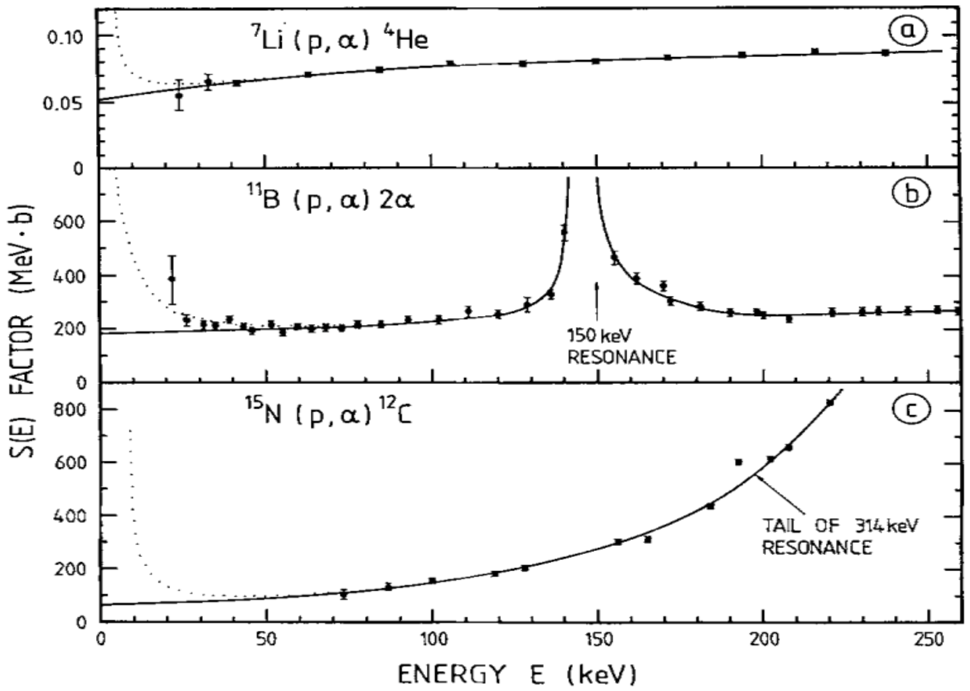

Effects of electron screening on low-energy fusion cross sections Assenbaum, H. J., Langanke, K., & Rolfs, C. 1987

ELECTRON SCREENING AND THERMONUCLEAR REACTIONS E. E. SALPETER 1954

$$R_D = 2.812x10^{-7}\rho^{-1/2}T_9^{1/2}\zeta^{-1}\ (cm)$$
$$Weak\ screening: R_D \gg r_{nuclei}\quad (stars)$$
$$Intermediate\ screening: \langle E_C\rangle \approx KT$$
$$Strong\ screening: \langle E_C\rangle \gg KT$$

$$f(E) = \frac{\langle\sigma_s v\rangle}{\langle\sigma_b v\rangle} \approx e^{\frac{\pi\eta U}{E}},$$
$$U \approx \frac{Z_1 Z_2 e^2}{R_o}$$
$$\sigma_{stdexp} \neq \sigma_{plasma} \approx \sigma_{stars} \neq \sigma_b = \sigma_{THM}$$

Coulomb Explosion of cryoclusters

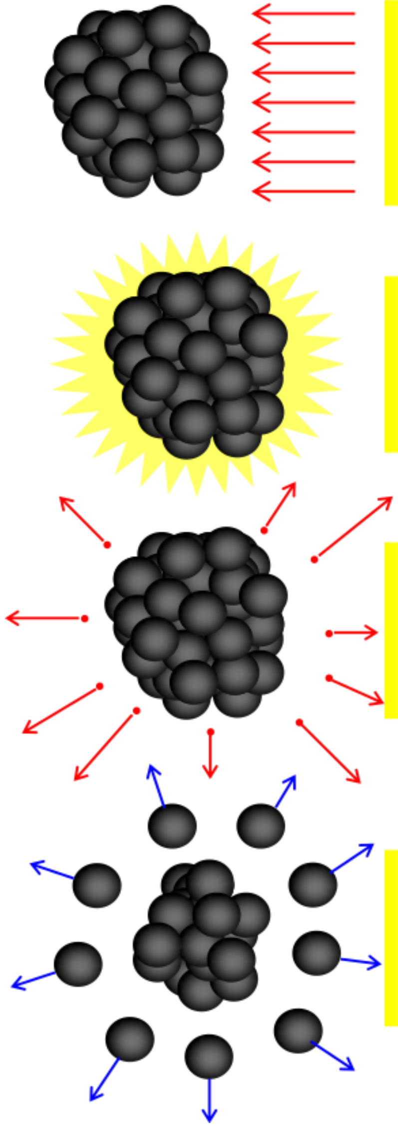

Step 1

Clusters are irradiated by high intensity laser pulse (~10^{16}~10^{18} W/cm^2).

Step 2

Laser pulse energy is first absorbed by electrons via heating mechanisms such as rapid collisional heating.

Step 3

Electrons escape from the cluster and leave positive charge build-up on the cluster.

Step 4

The cluster "explodes" and deuterons acquire multi-keV kinetic energy.

Exp. Campaigns @ UT Petawatt Laser 2011&2016

E = 100-140 J
Pulse duration: 140 fs
Rep. Rate: ~ 1/hour
CW: 1057 nm
Intensity ~ 10^{21} W/cm^2

$$d + d \rightarrow {}^3\mathrm{He}(0.82MeV) + n(2.45MeV)$$

$$d + d \rightarrow p(3.02MeV) + t(1.01MeV)$$

$$d + {}^3\mathrm{He} \rightarrow p(14.7MeV) + {}^4\mathrm{He}(3.6MeV)$$

deuterium ions
Kinetic Energy: 1-10^2 keV
Density ~ 10^{18} atoms/cm^3
10^5 – 10^7 neutrons per shot

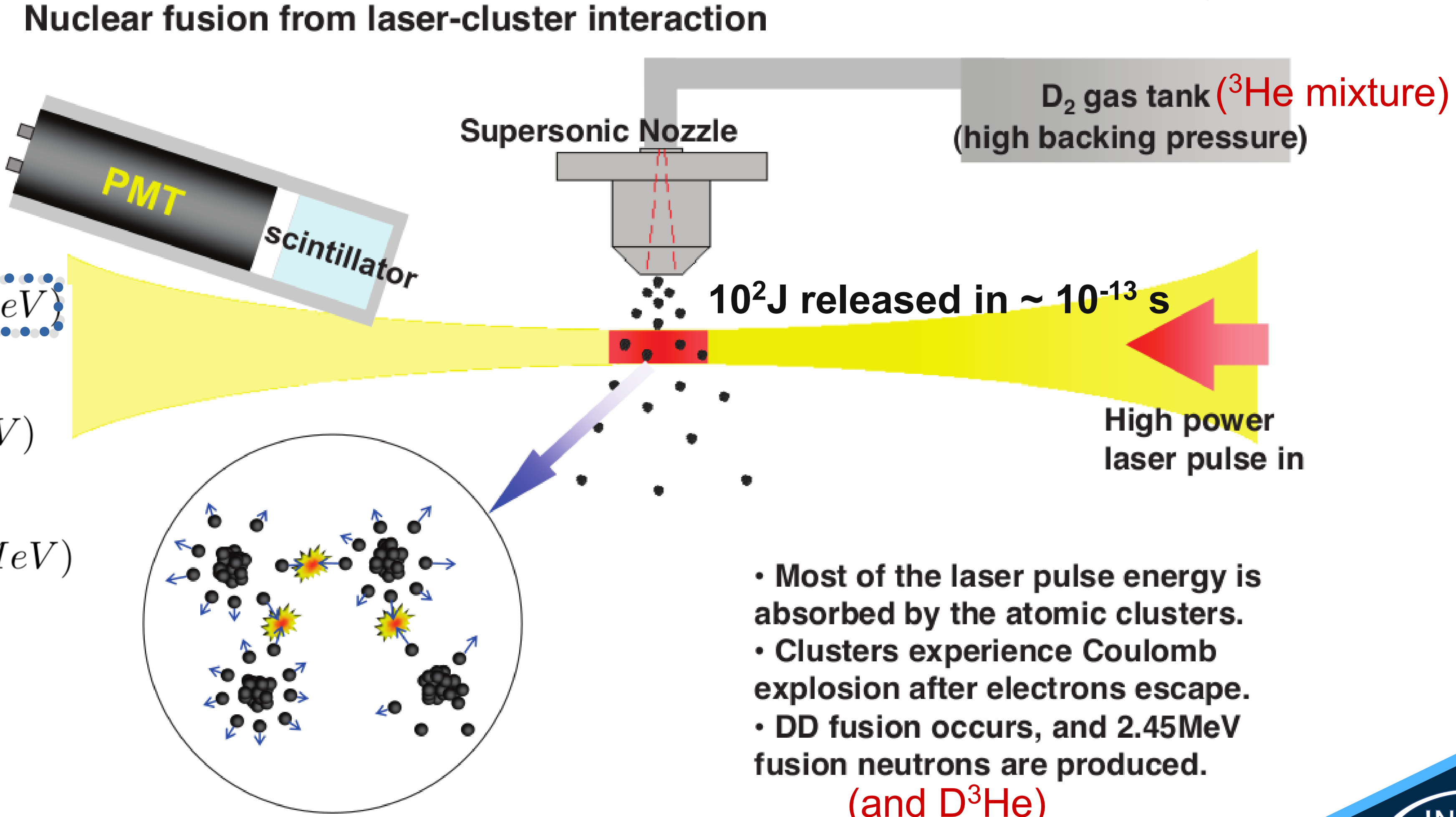

- Most of the laser pulse energy is absorbed by the atomic clusters.
- Clusters experience Coulomb explosion after electrons escape.
- DD fusion occurs, and 2.45MeV fusion neutrons are produced. (and D^{3}He)

Ditmire T. et al., Nuclear fusion from explosions of femtosecond laser-heated deuterium clusters. Nature 398, 489–492 (1999);
Ditmire T. el al., Nuclear fusion in gases of deuterium clusters heated with a femtosecond laser, Physics of Plasmas 7, 1993 (2000);
Bang W., et al., Temperature Measurements of Fusion Plasmas Produced by Petawatt-Laser-Irradiated D2−3He (…) Clustering Gases, Phys. Rev. Lett. 111, 055002 (2013)
Barbui M. el al, Measurement of the Plasma Astrophysical S Factor for the 3He(d,p)4He Reaction in Exploding Molecular Clusters, Phys. Rev. Lett. 111, 082502 (2013);
Lattuada D. et al, Model-independent determination of the astrophysical S factor in laser-induced fusion plasmas, Phys. Rev. C 93, 045808 (2016).
Quevedo H., et al, Neutron enhancement from laser interaction with a critical fluid Physics Letters, Section A, 382 (2-3), (2018).

$$d + d \rightarrow {}^3\mathrm{He}(0.82MeV) + n(2.45MeV)$$

$$d + {}^3\mathrm{He} \rightarrow p(14.7MeV) + {}^4\mathrm{He}(3.6MeV)$$

$$Y_{n,BB} = l\rho_D \int \frac{dN}{dE} \sigma_{BB}(E) dE$$

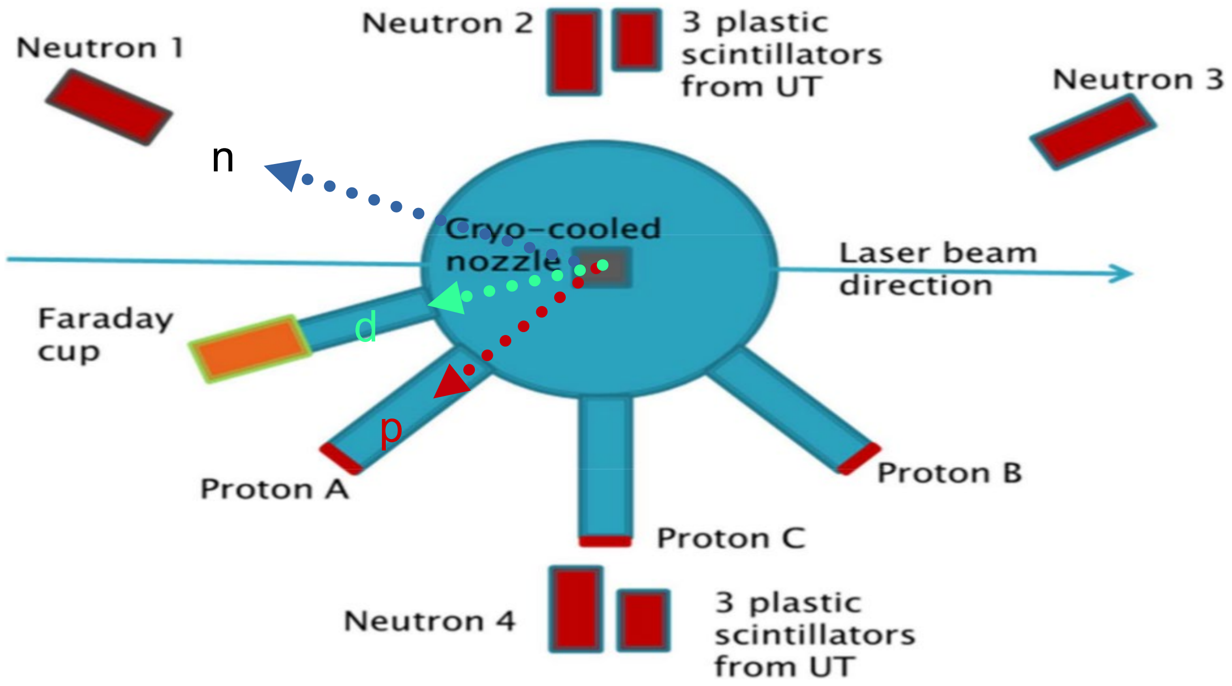

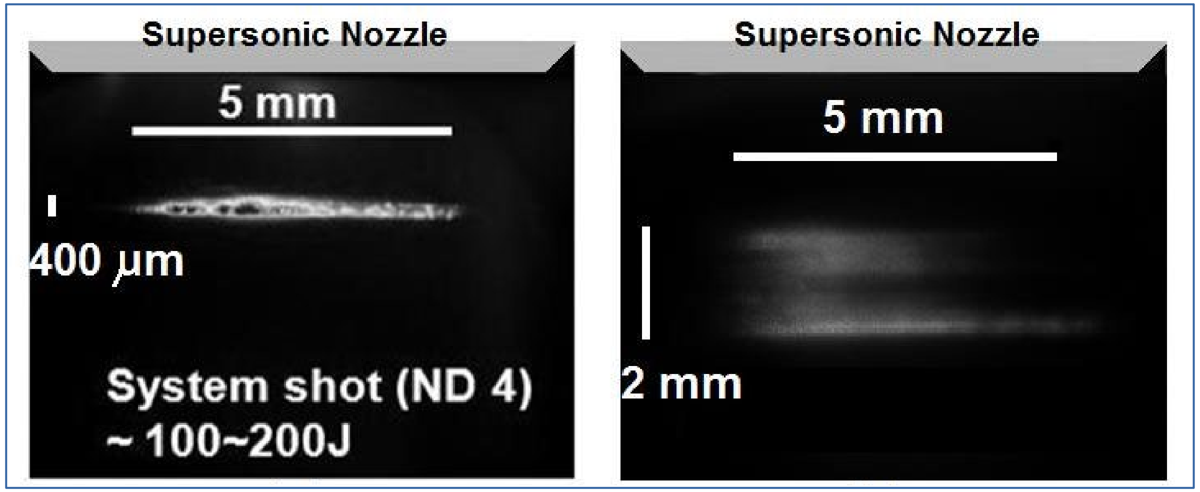

Signals and results

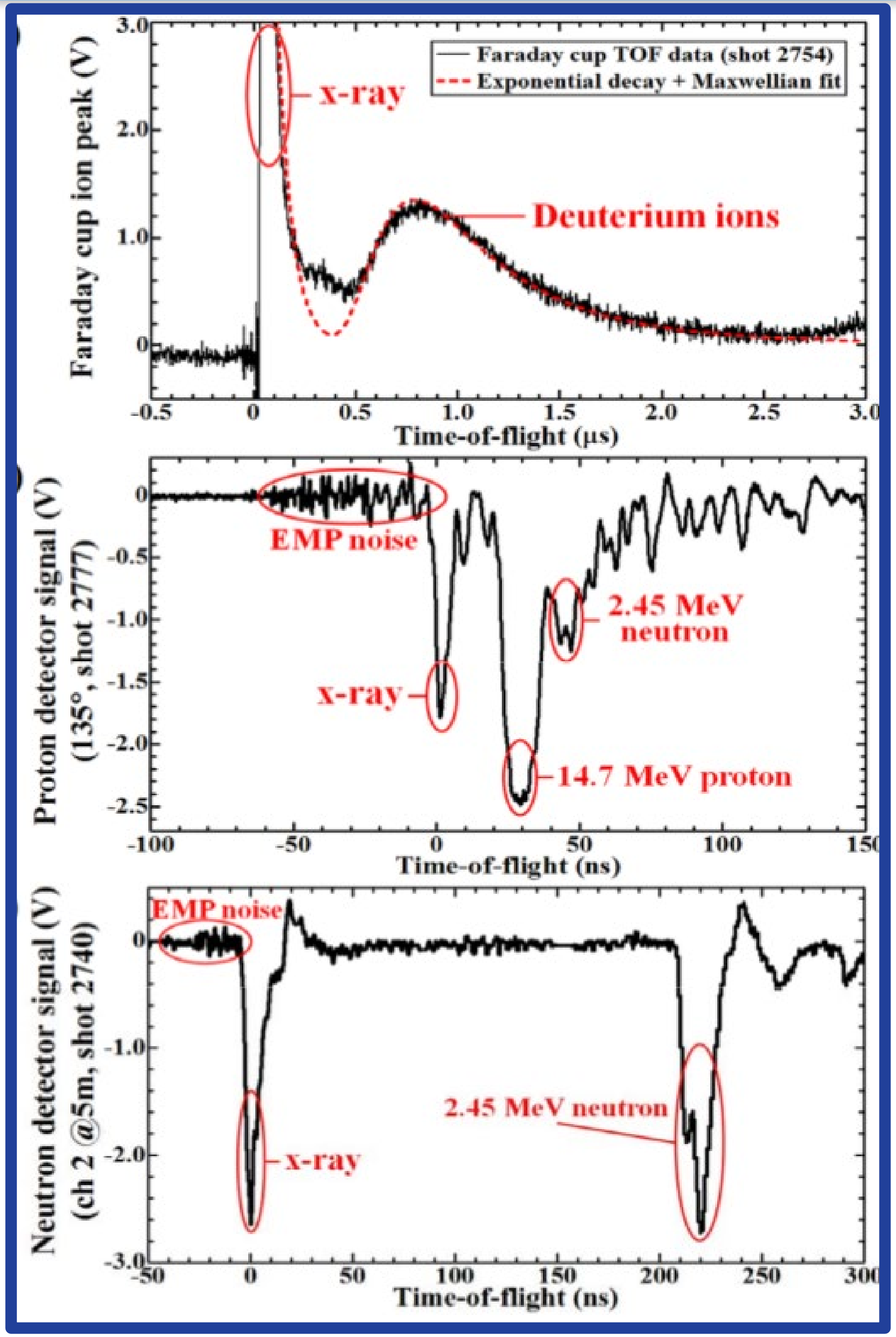

$$Y_{n,BB} = l\rho_D \int \frac{dN}{dE}\sigma_{BB}(E)dE$$

$$\sigma(E) = \frac{S(E)}{E}\exp(-2\pi\eta(E))$$

$$2\pi\eta = b/\sqrt{E}$$

$$b = 0.9898 Z_i Z_j \sqrt{A}\ \mathrm{MeV}^{1/2}$$

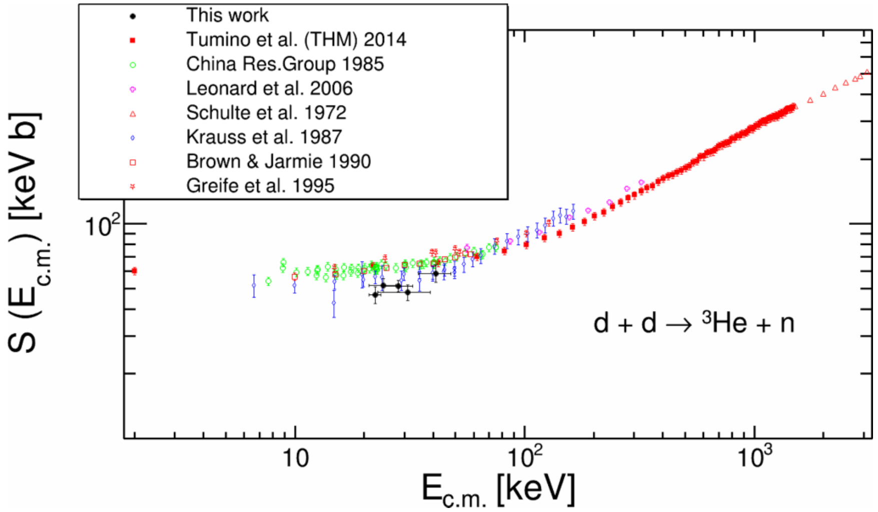

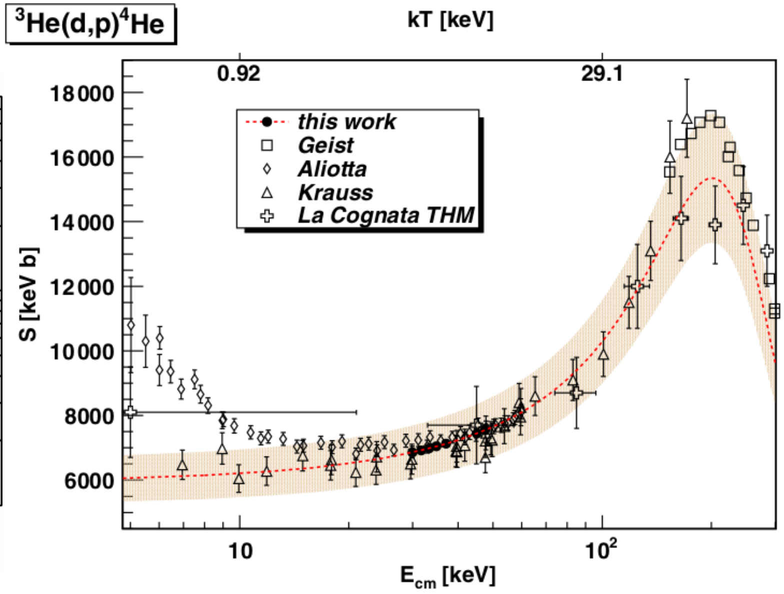

Versatile Array for Laser-induced Astrophysics Research

- *Science-driven, portable, cost-efficient*

- cryo-cooled supersonic nozzle
- compact interaction chamber
- neutron ToF detectors (plastic/liquid scintillators)
- charged particle ToF detectors (SiC/CVD diamond detectors + FCs)
- 2 TPS with MCP readout
- CR39 supplies and ancillary equipment

- *additional R&D:*
- ɣ & e^- calorimeters, TimePix3, MCP as ToF

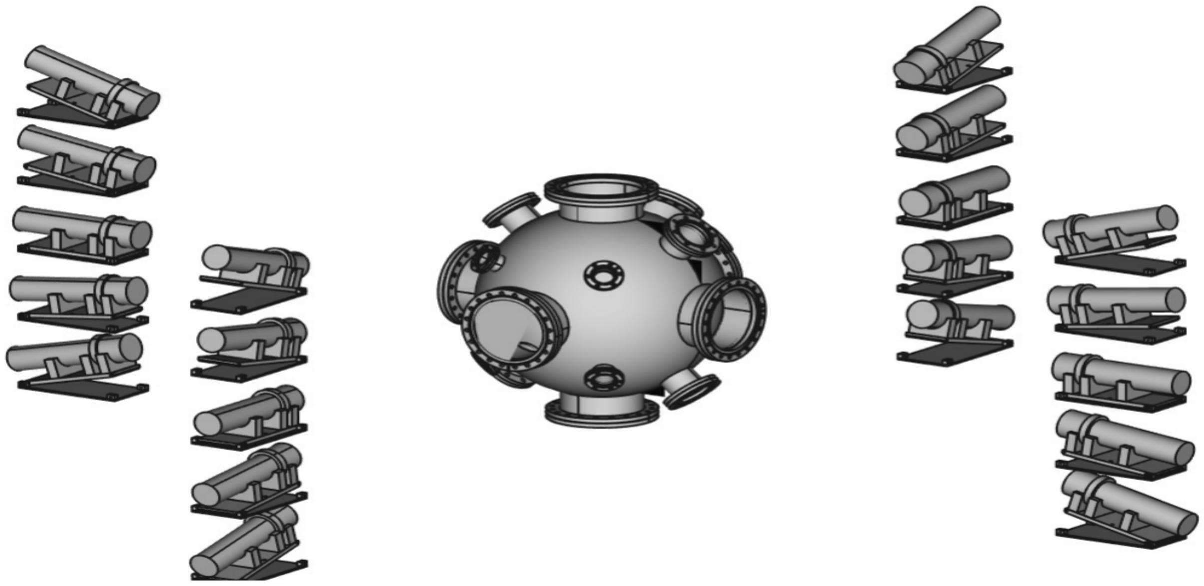

Under evaluation by funding agencies

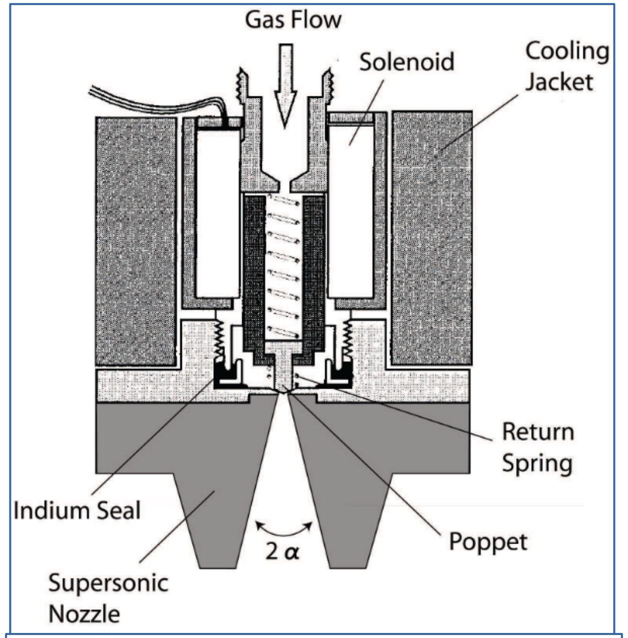

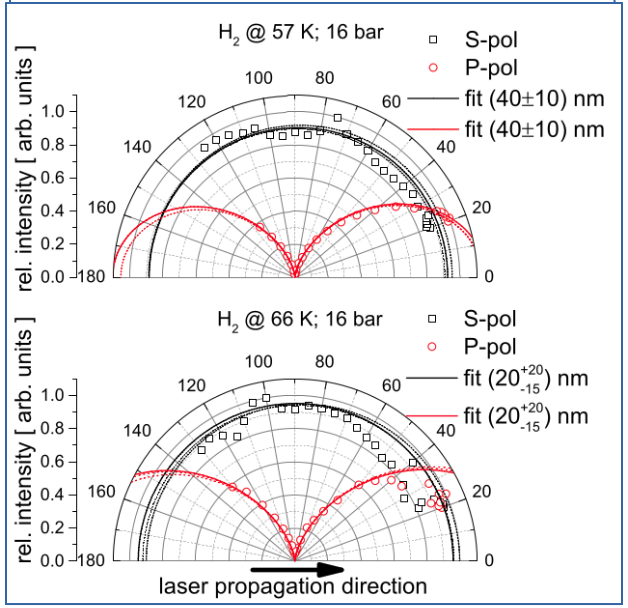

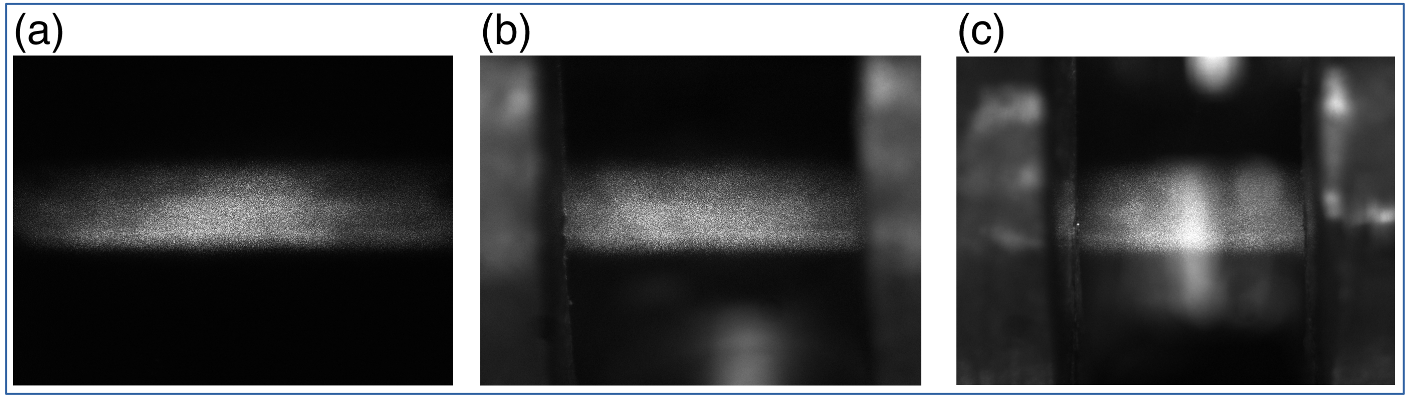

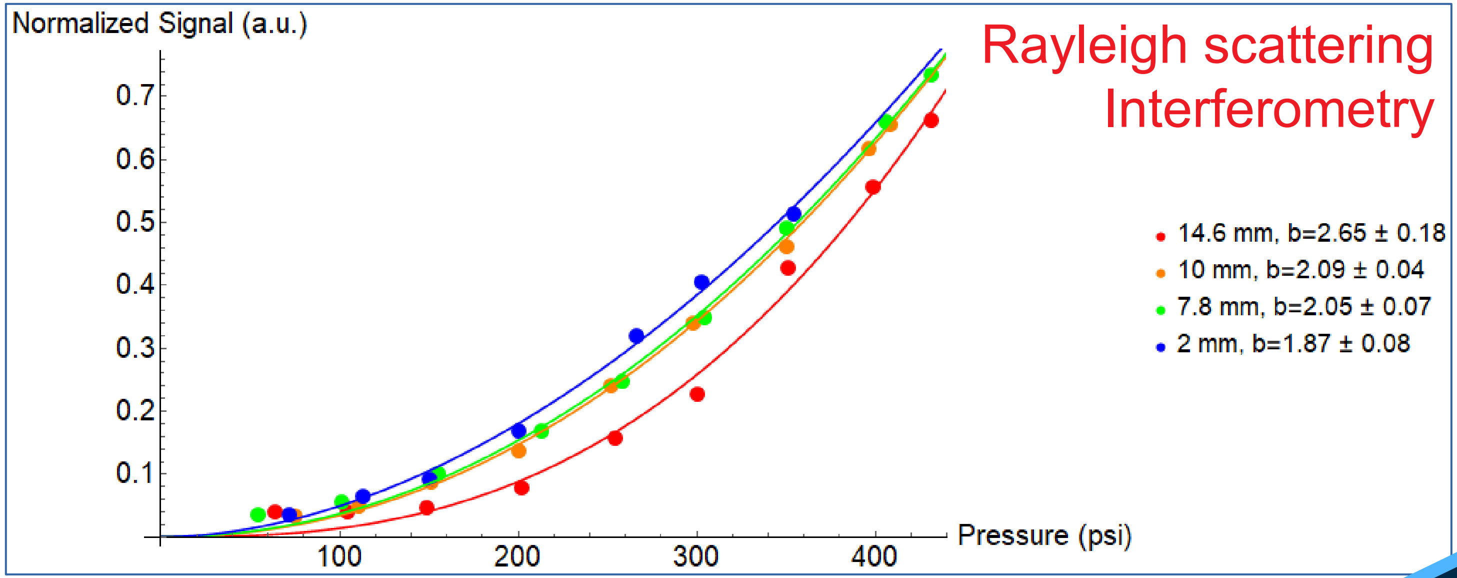

S. Grieser, Nm-sized cryogenic hydrogen clusters for a laser-driven proton source Rev. Sci. Instrum. 90, 043301 (2019)
G.D. Glenn, Thesis @ University of Texas at Austin (2019)

The ToF neutron detectors

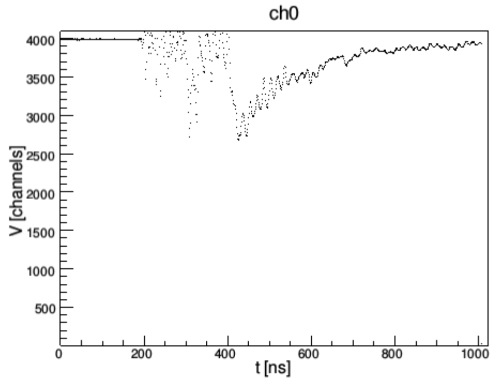

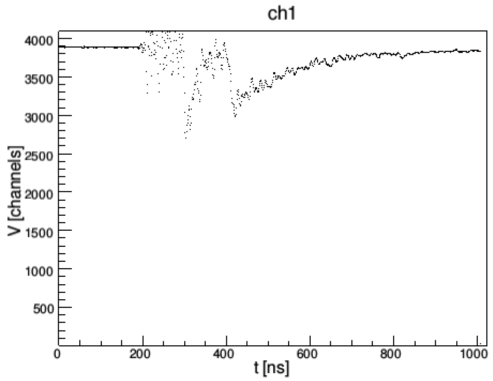

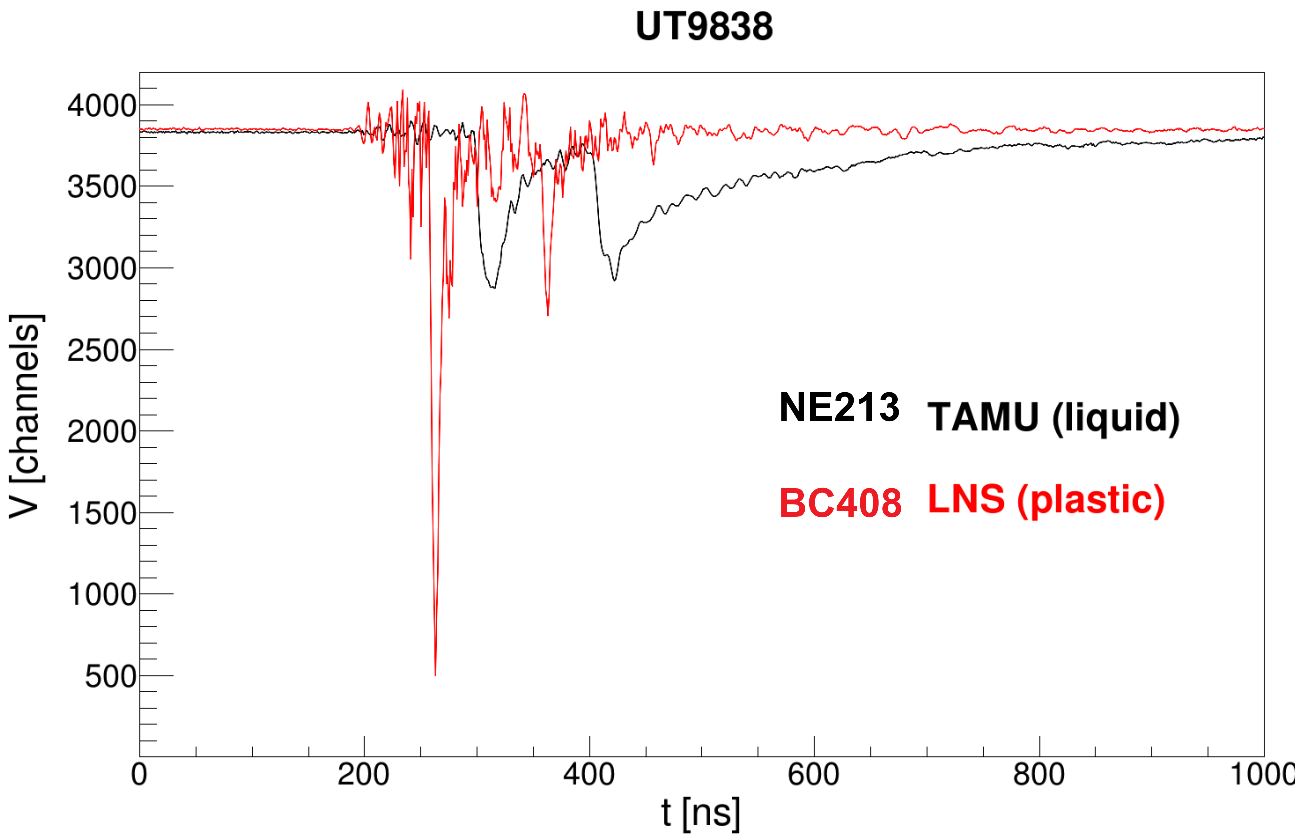

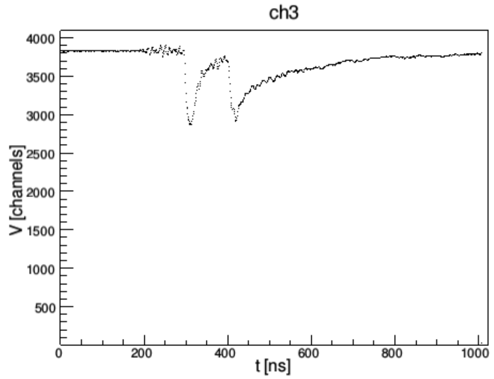

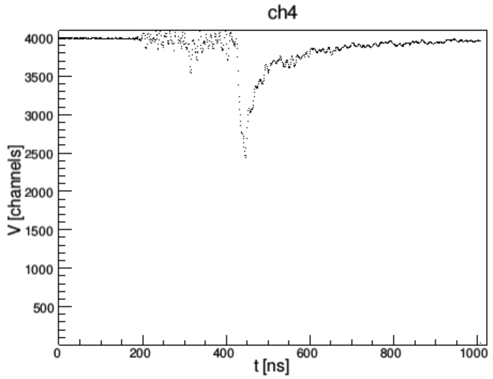

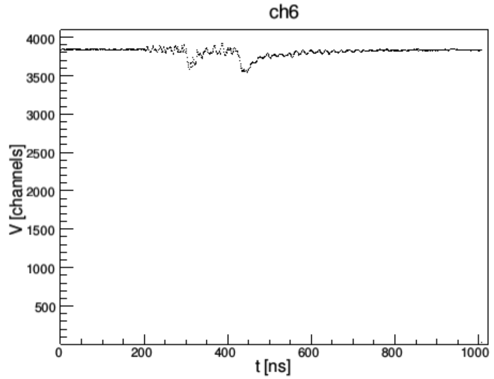

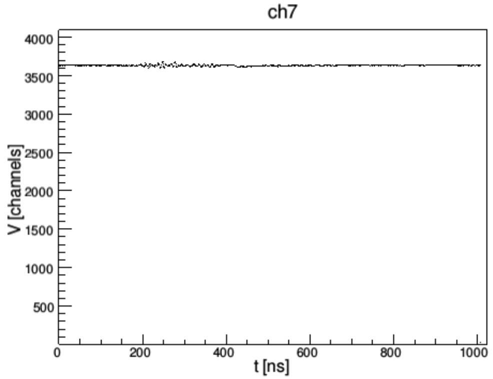

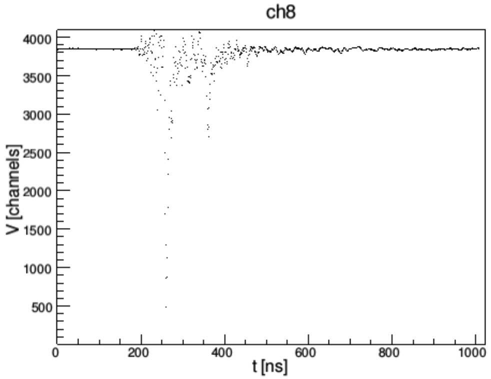

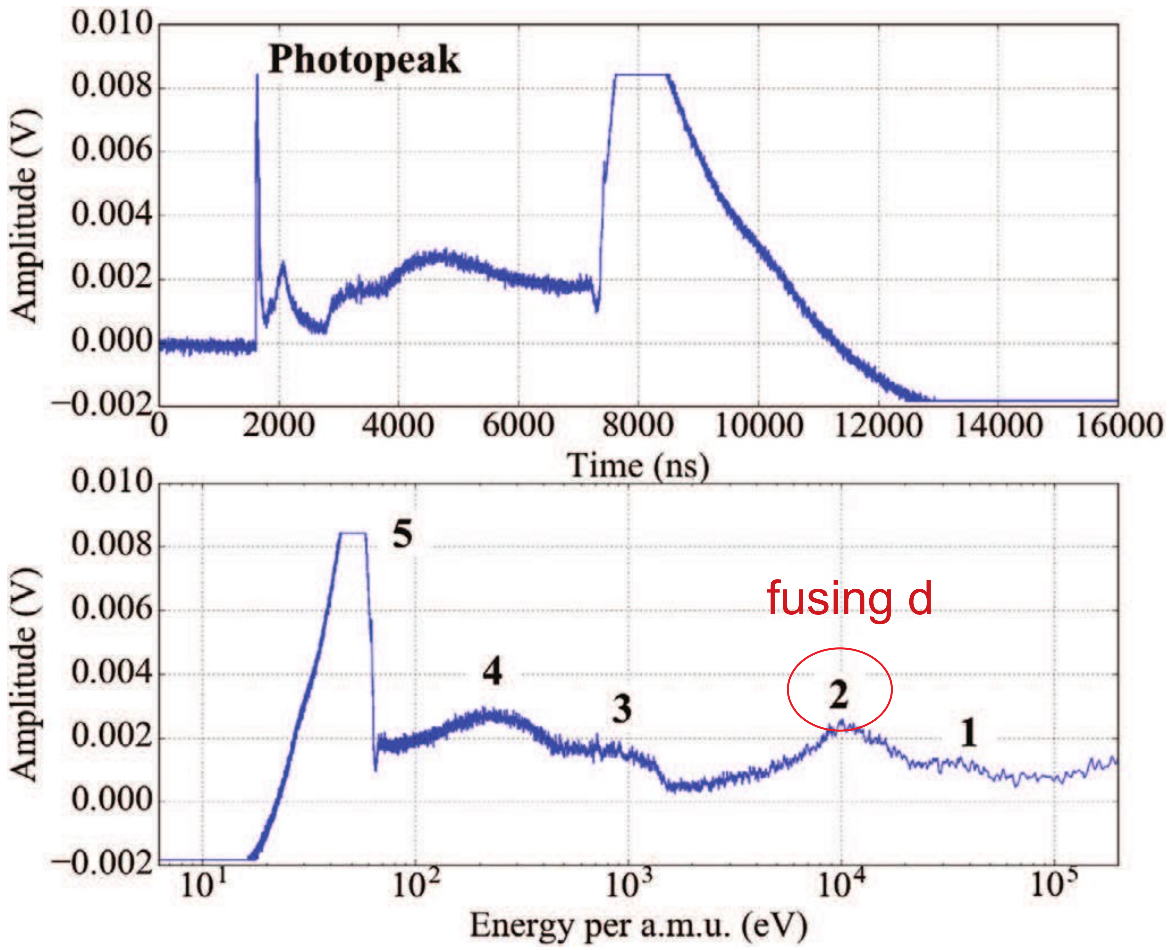

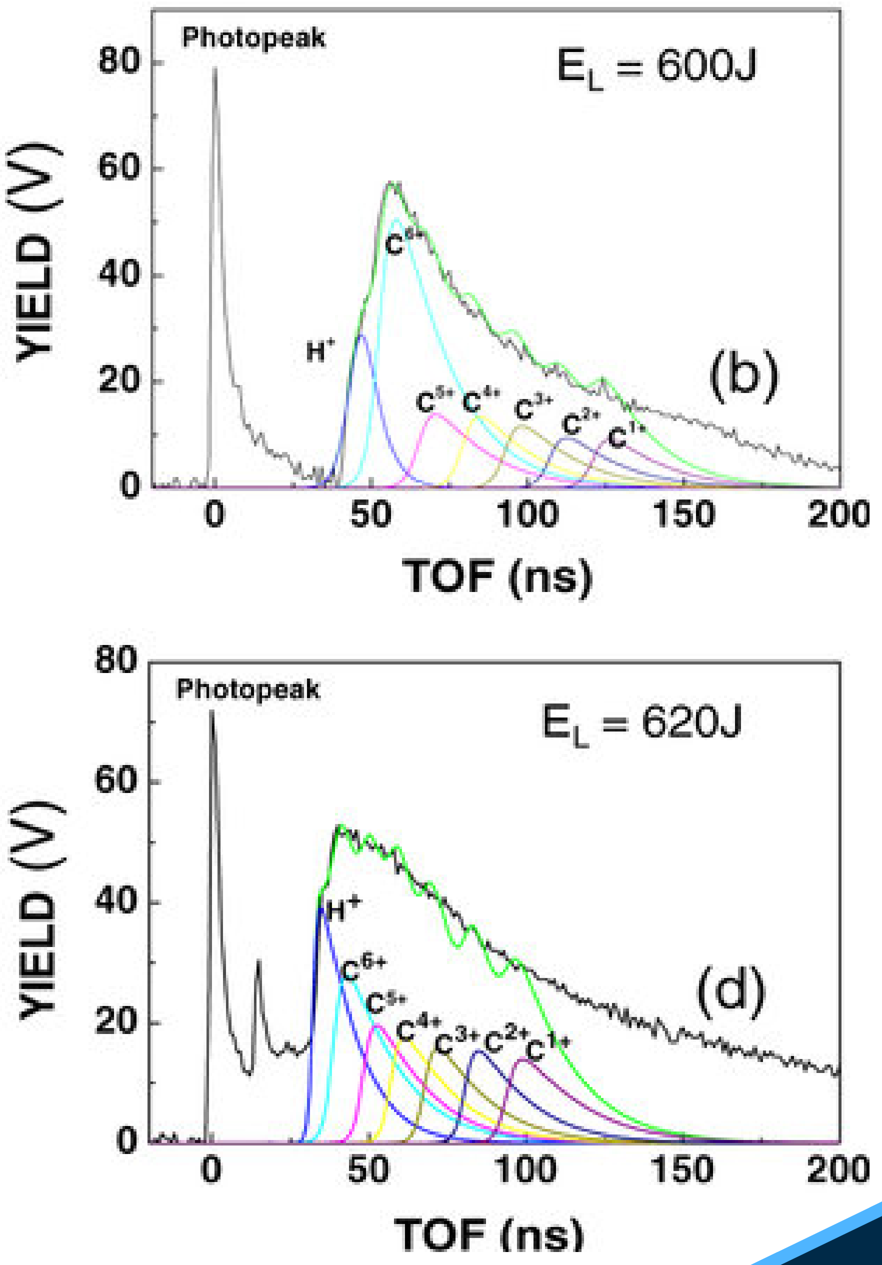

Silicon carbides

Mono-crystalline CVD diamonds

D. Giulietti et al., D+D fusion reactions in 10^{18} W/cm^2 intensity and repetitive laser-plasma interactions, EPL, 119 (2017)

P. Musumeci et al., Silicon carbide detectors for diagnostics of ion emission from laser plasmas, Physica Scripta T161 (2014)

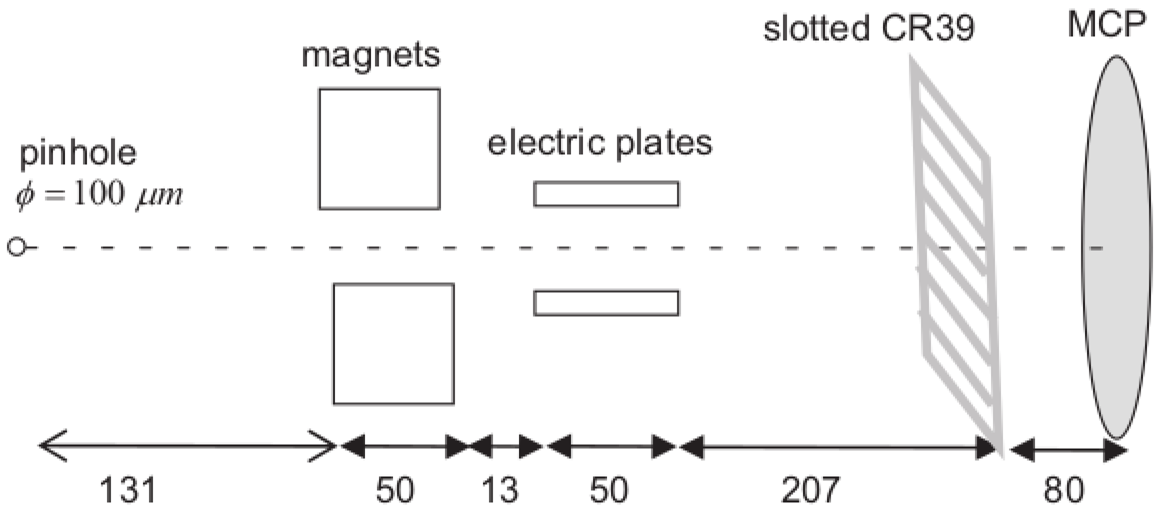

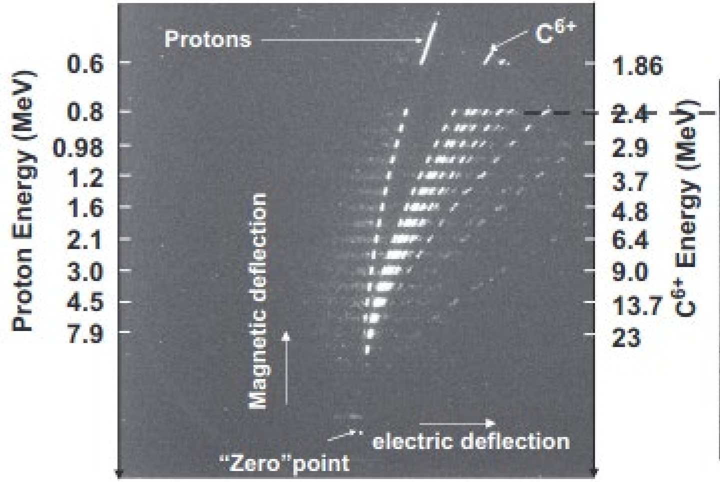

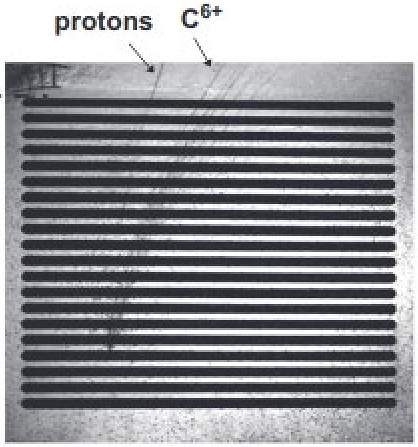

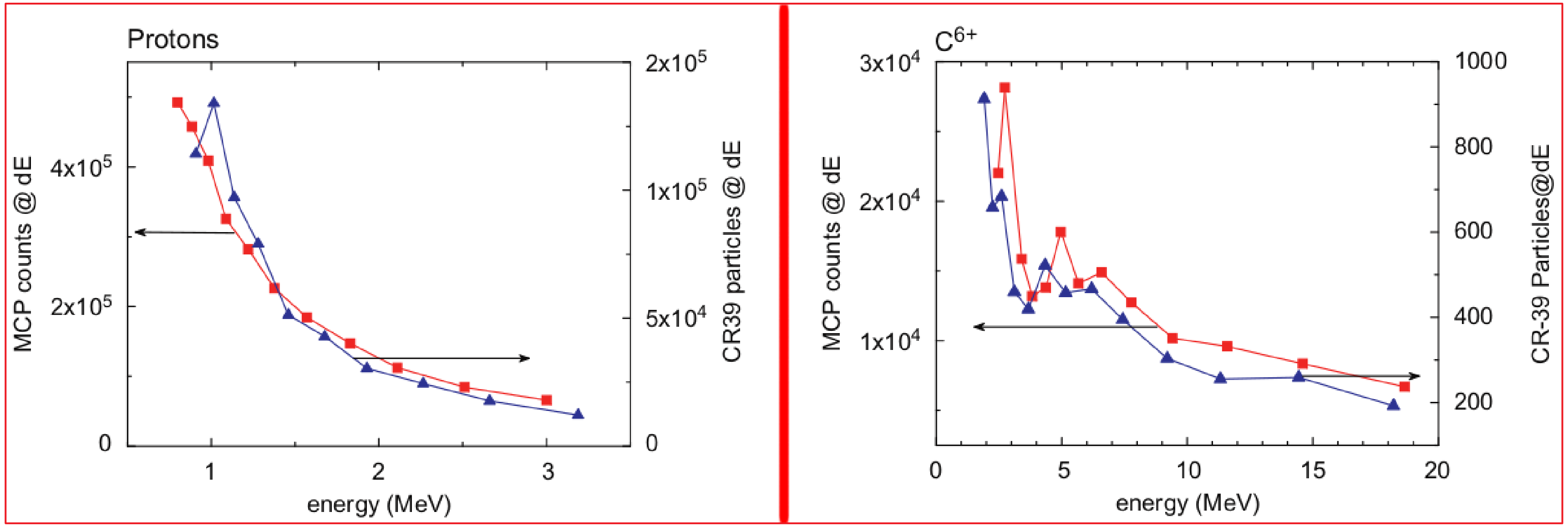

IP, MCP, CMOS ..

R. Prasad et al., Calibration of Thomson parabola—MCP assembly for multi-MeV ion spectroscopy, Nuclear Instruments and Methods in Physics Research A 623 (2010)

"Facilities" @LNS and @LNF

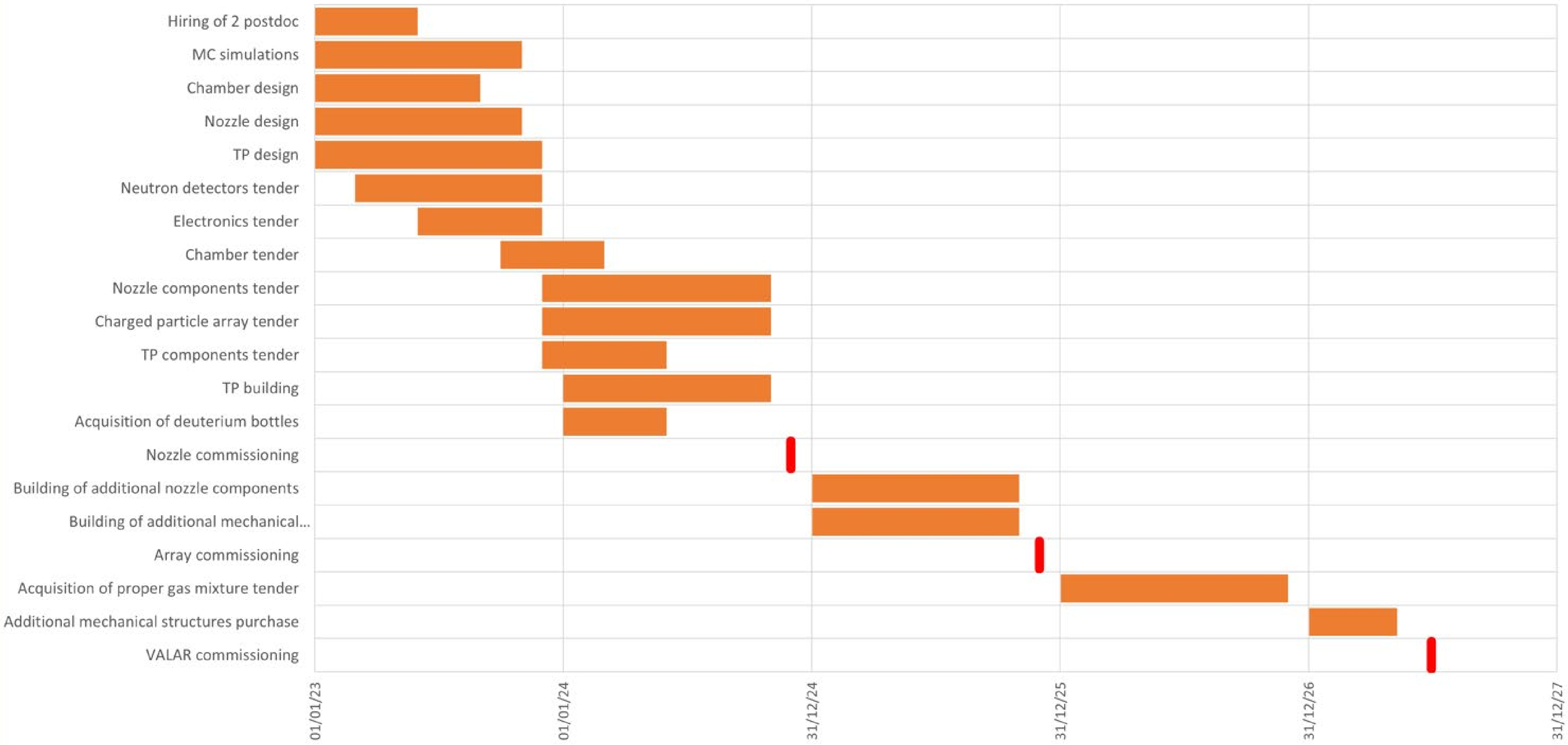

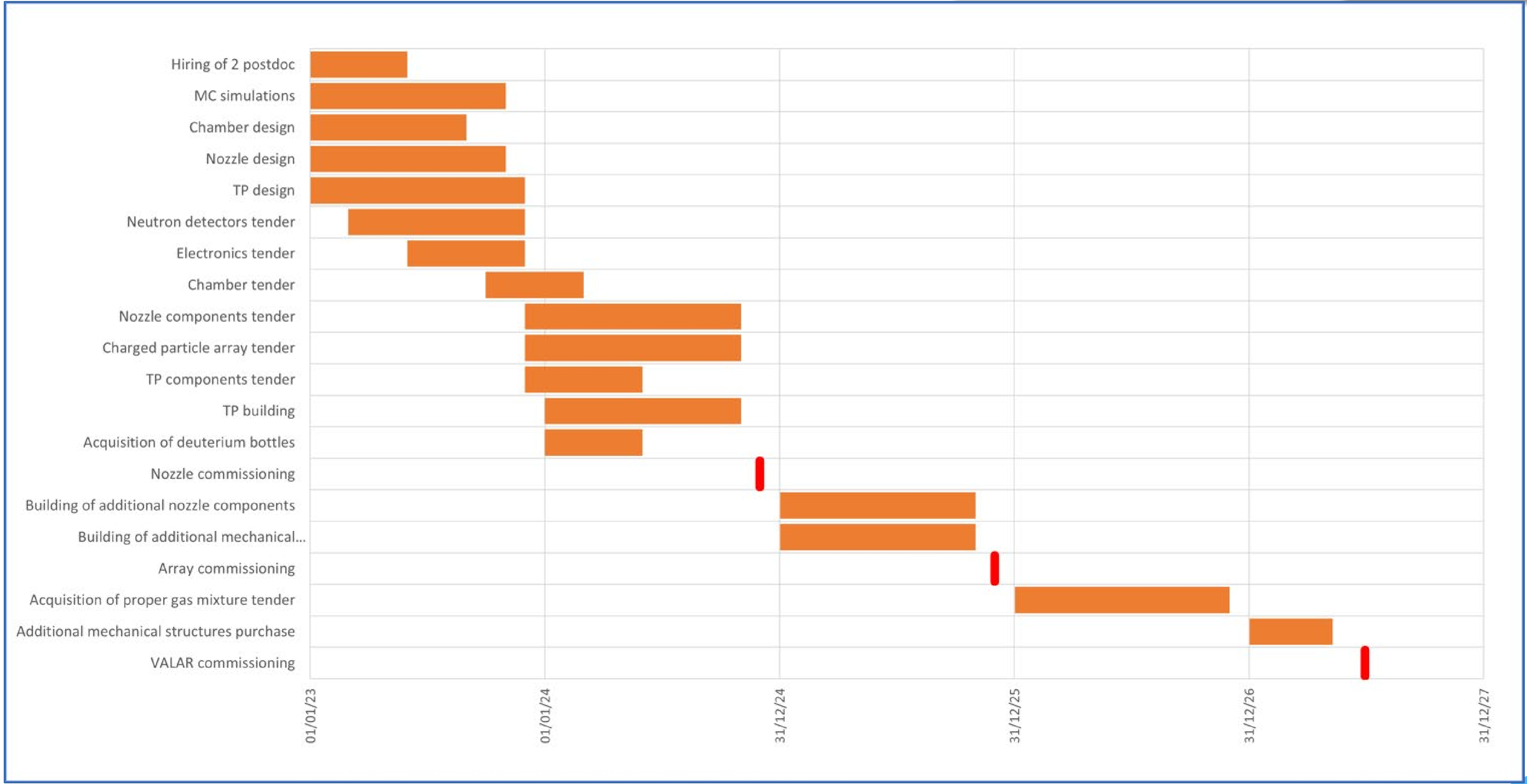

Graphic designer for the LOGO somewhen here

Ok, where?

“Facilities” @LNS and @LNF

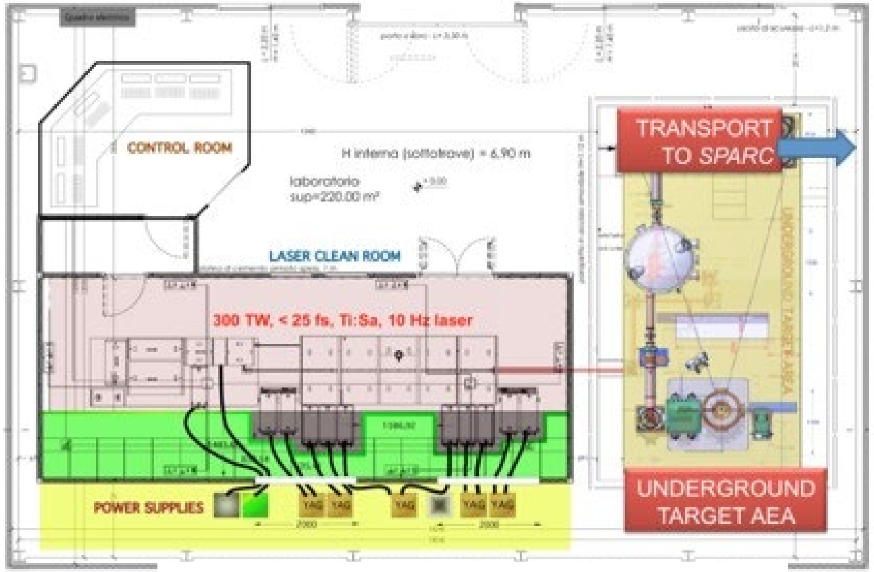

eli nuclear physics

E4:	100TW	22-100fs	2.2J	10Hz
E5:	1PW	24-1000fs	25J	1Hz
HPLS:	(2x) 10PW	25fs	10^2J	1/hour

CENTER FOR HIGH ENERGY DENSITY SCIENCE

TPW:	1PW	140fs	140J	1/hour

CLPU CENTRO DE LÁSERES PULSADOS

VEGA1:	100TW	30fs	0.6J	10Hz
VEGA2:	200TW	30fs	6J	10Hz
VEGA3:	1PW	30fs	30J	1Hz

INFN
Istituto Nazionale di Fisica Nucleare

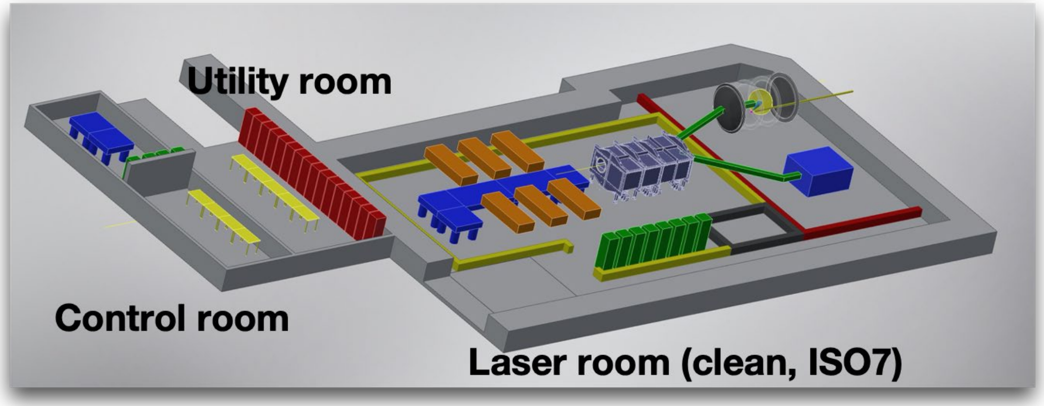

I-LUCE facility

I-LUCE: INFN Laser IndUced particle acCeleration

aim: electron, proton acceleration; nuclear reaction in warm dense matter; ion-plasma interaction studies

Peak power : 1 PW
Pulse duration: <25fs
Repetition rate: 1 Hz
System designed to be upgradable up to 1 PW

→

Max energy
protons: 150 MeV
electrons: 8 GeV

Funds:

EuAPS	I-LUCE for Breast Cancer Therapy	SAMOTHRACE (Sicilian Micro and Nano Technology Research and Innovation Center)
7.9 M€	2.5 M€	1 M€


Beamlines
Text
Officies
Laser-area
Cyclotron
Tandem accelerator
INFN
Istituto Nazionale di Fisica Nucleare

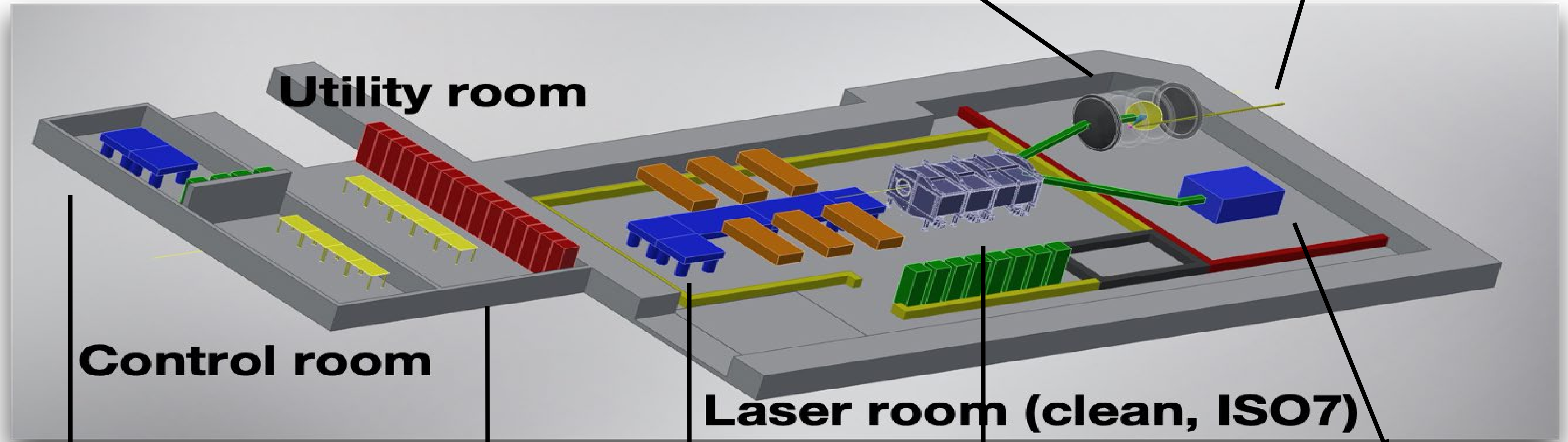

Plasma–ion interaction chamber; Plasma and nuclear physics studies

Ion beams from Cyclotron and Tandem

Proton-, ion– and electron acceleration

Optical laboratory

Pumps laser bias supplies

Laser system

Laser compressor chamber

1st Phase

Laser tender is starting (2022)

Middle 2024 the first experimental station

Two laser lines and three experimental stations:

Fusion studies

Acceleration

Plasma-ion interaction

Laser Power	~ 1 TW
Energy per pulse	25-30 mJ
Pulse duration	25-30 fs*
Contrast ratio ns	< 1*10-8
Contrast ratio @5 ps	> 10^5
Contrast ratio @100 ps (ASE)	> 10^{10}
Repetition rate	10 Hz

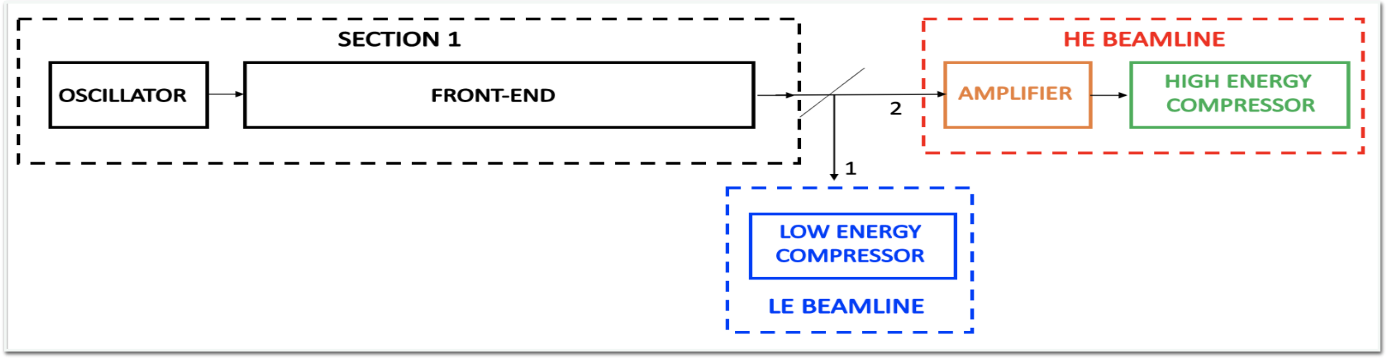

Laser Power	50-250 TW
Energy per pulse	≥ 1-10 J
Pulse duration	<= 25 fs
Contrast ratio ns	> 10^8
Contrast ratio @5 ps	> 10^5
Contrast ratio @100 ps (ASE)	> 10^{10}
Repetition rate	1 Hz
Path to upgrade up to 1PW	Compressor optics ready for the upgrade up to 1PW
Pointing stability	<50 µrad
Beam diameter (FWHM)	50-60 mm
Strehl ratio	>=0.65 (without deformable mirror) >=0.8 (with deformable mirror)

2nd Phase

Laser tender will start in 2023

At the end of 2025 the first call for external users

- **proton, ion, electron acceleration;**
- **biological experiments;**
- **neutrons and gamma production;**
- **ion-plasma interaction;**
- **nuclear studies in plasma**

Laser Power	1 PW
Energy per pulse	≥ 25 J
Pulse duration	<= 25 fs
Contrast ratio ns	> 10^8
Contrast ratio @5 ps	> 10^5
Contrast ratio @100 ps (ASE)	> 10^{10}
Repetition rate	1 Hz
Path to upgrade up to 1PW	Compressor optics ready for the upgrade up to 1PW
Pointing stability	<50 µrad
Beam diameter (FWHM)	50-60 mm
Strehl ratio	>=0.65 (without deformable mirror) >=0.8 (with deformable mirror)

- √ **Proton, electron and neutron sources**
- √ **Free Electron Laser radiation**
- √ **Dosimetry and Radiobiology** of «FLASH» beams (electrons, protons, gamma)
- √ **Cultural Heritage:** PIXE studies with laser-driven protons
- √ **Space applications:** laser-driven beams could easily reproduce the space radiation quality
- √ **Radioisotopes production:** laser-driven beams could easily produce high intensity charged particles beams
- √ Imaging at the molecular level with **ultrafast X-Rays** (ex radiation chemistry of the radiolysis)
- √ **Stopping powers** in plasma
- √ Studies on **Nuclear Reactions** in plasma with particular focus on the pB reaction* (PROBONO Cost Action)
- √ Materials studies
- √ MORE..

Ion-plasma interaction:
UNIQUE CAPBILITY OF INFN-LNS

FLAME @ SPARC_LAB

- ***FLAME itself***

a. Electron acceleration by self injection
b. Light ion acceleration by TNSA
c. Air propagation by LIDAR

- ***FLAME + SPARC***

a. Compton scattering
b. Electron acceleration by external injection

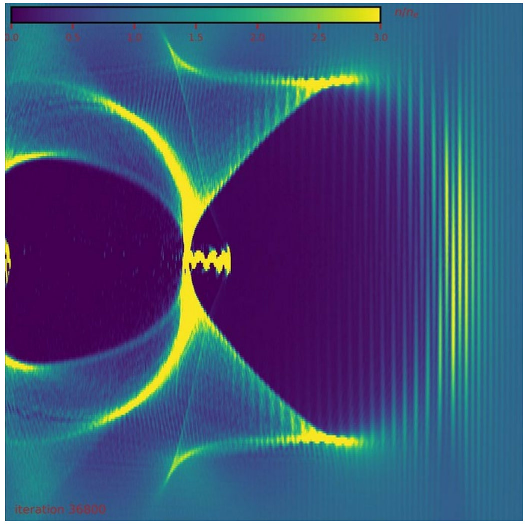

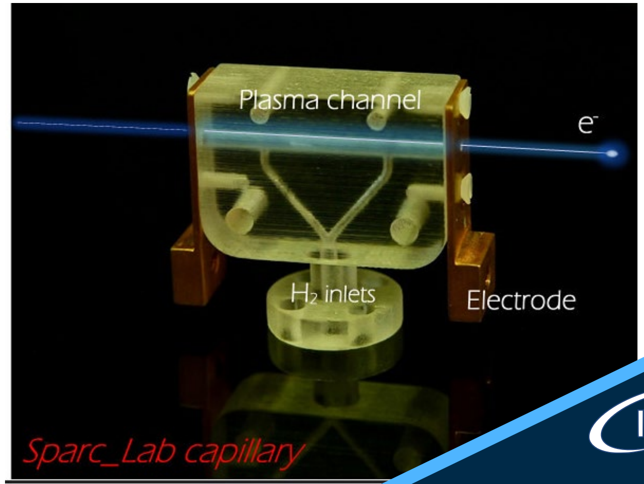

Massimo Ferrario, Maria Pia Anania.

FLAME

Max energy: 7J

Min bunch duration: 23 fs

Wavelength: 800 nm

Spot-size @ focus: 10 μm

Max power: 300 TW

Contrast ratio: 10^{10}

Intensity: 10^{19} W/cm^2 (→10^{21})

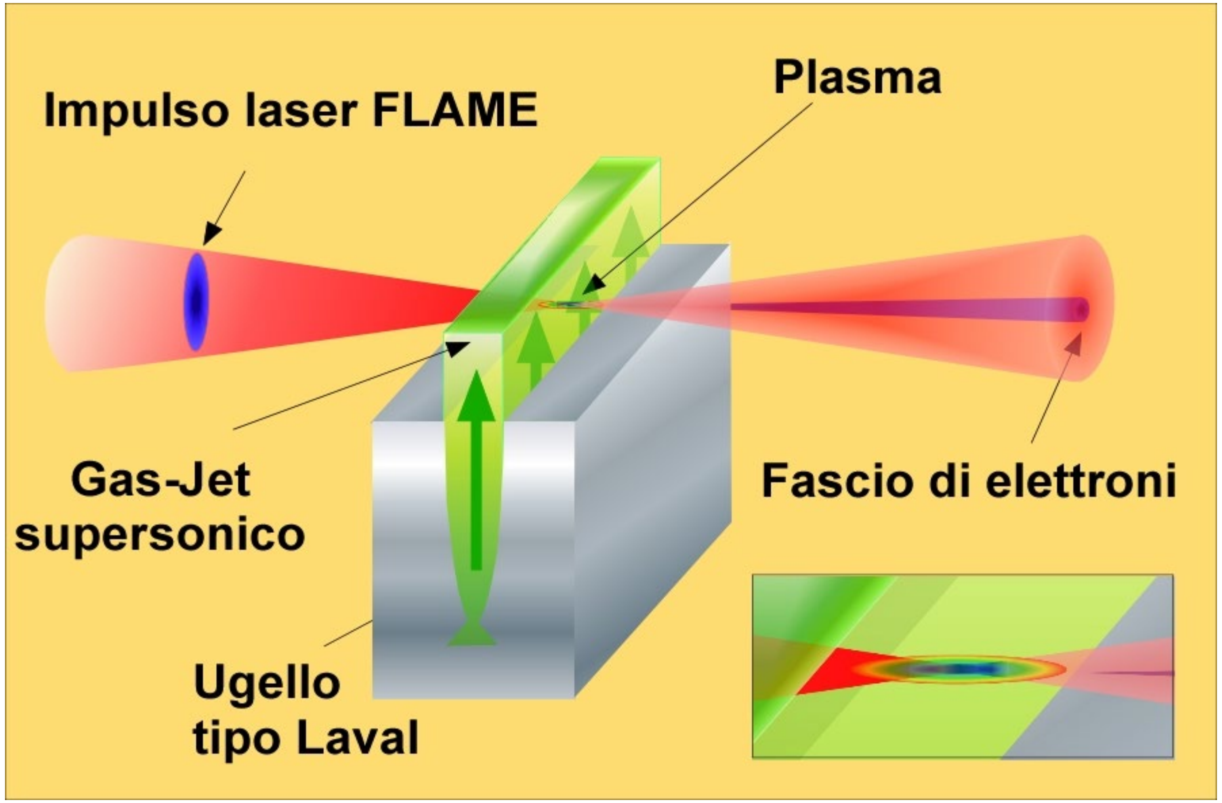

Laser wakefield accelerators (LWFA) are a novel type of accelerators capable to produce accelerating field up to 100 GV/m. This feature gives the possibility to have very compact accelerators able to accelerate electrons to GeV energies in few **centimetres**.

FLAME

Max energy: 7J

Min bunch duration: 23 fs

Wavelength: 800 nm

Spot-size @ focus: 10 μm

Max power: 300 TW

Contrast ratio: 10^{10}

Intensity: 10^{19} W/cm^2 (→10^{21})

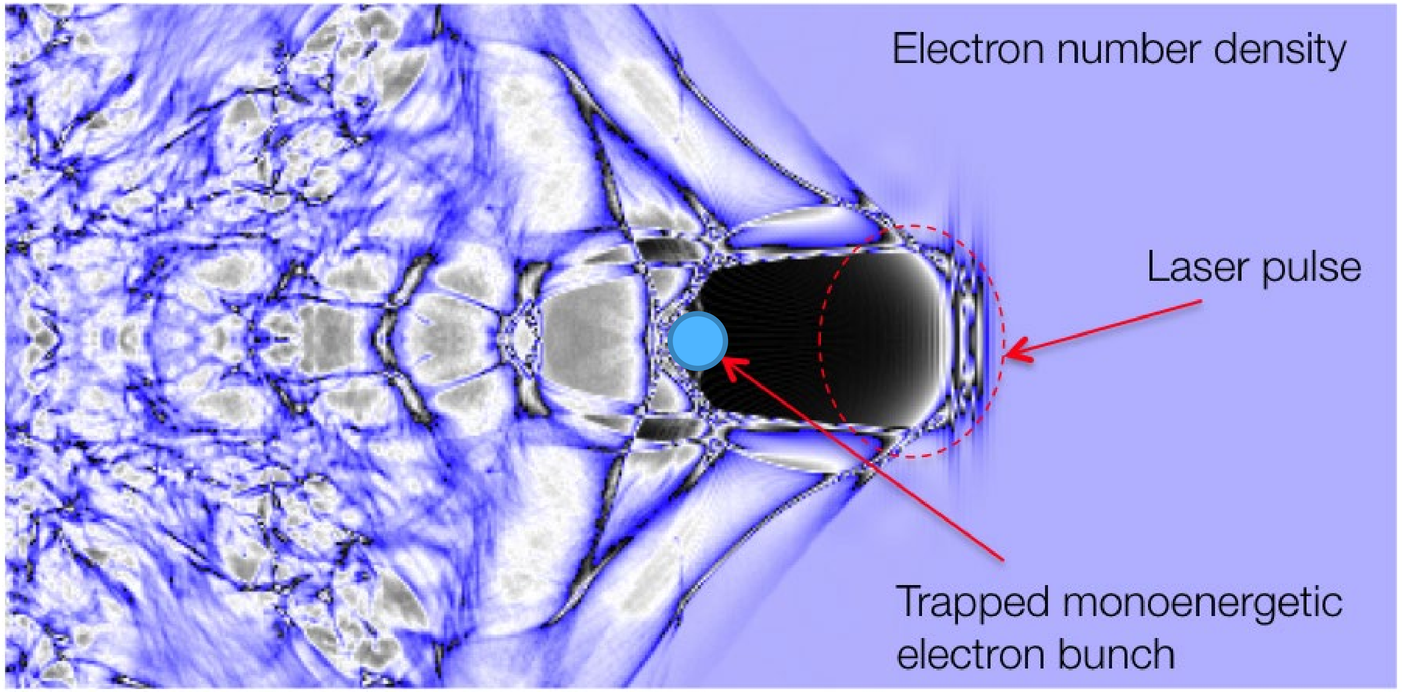

External injection: electrons accelerated by the linac injected with the right phase on the creast of the wakefield to be further accelerated. Electrons exit with a higher energy and a quality comparable to that of incoming electron beam.

EUPRAXIA

1st Phase: 500TW laser will be installed

2nd Phase: second 500TW (or upgrade to 1PW)

Two 500TW laser could satisfy the 24h/7day operation request in parallel on different experiments.

	Units	value
Central wavelength	nm	800
Bandwidth	nm	60 - 80
Repetition rate	Hz	1 - 5
Max energy before compression	J	20
Max energy on target	J	13
Min pulse length	fs	25
Max power	TW	500
Contrast ratio		10^{10}
Laser spot size at focus (optics dependent)	μm	2 - 50
Peak power density at focus (optics dependent)	W/cm^2	10^{22} - 10^{19}

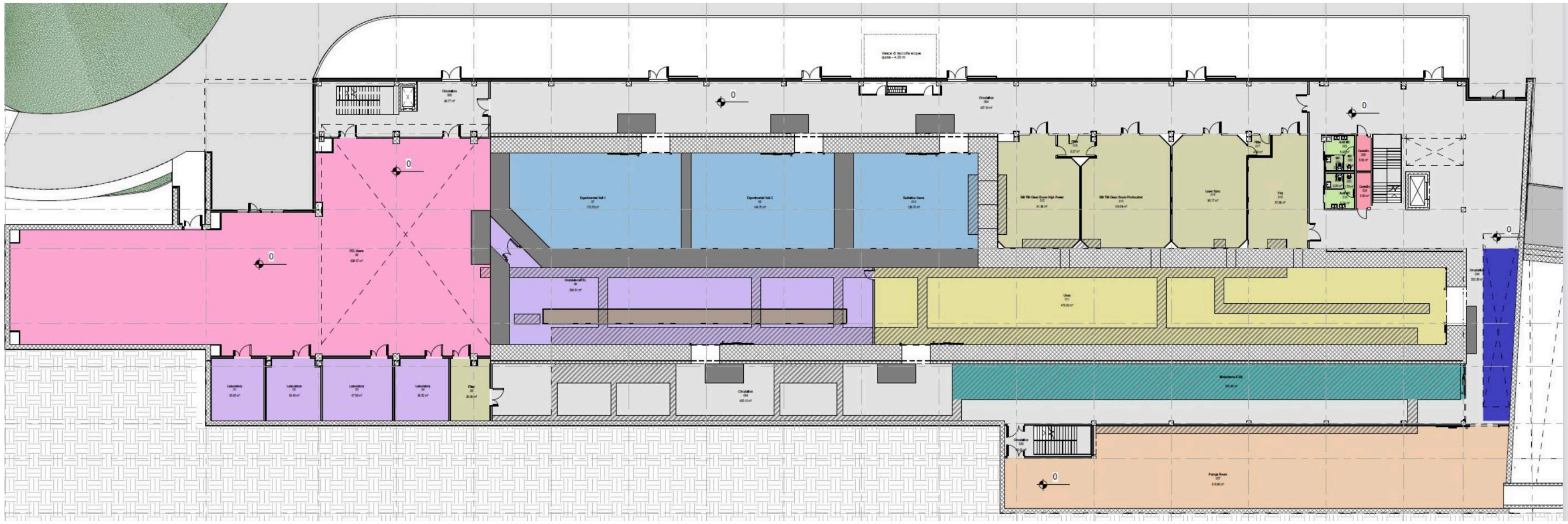

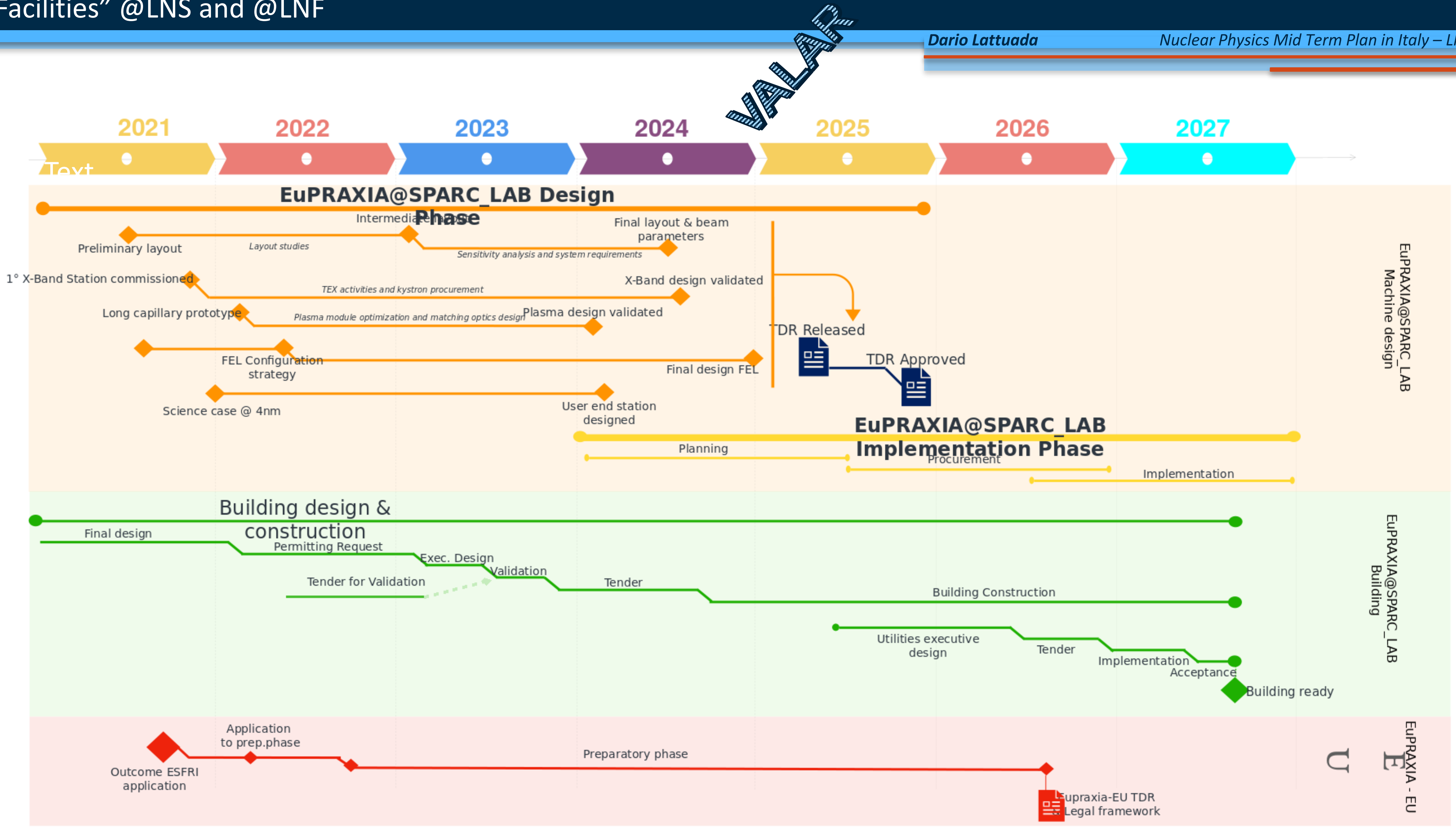
VALAR
2021
2022
2023
2024
2025
2026
2027
Text
EuPRAXIA@SPARC_LAB Design Phase
Intermediate layout
Final layout & beam parameters
Preliminary layout
Layout studies
Sensitivity analysis and system requirements
1° X-Band Station commissioned
TEX activities and kystron procurement
X-Band design validated
Long capillary prototype
Plasma module optimization and matching optics design
Plasma design validated
TDR Released
FEL Configuration strategy
Final design FEL
TDR Approved
Science case @ 4nm
User end station designed
EuPRAXIA@SPARC_LAB Implementation Phase
Planning
Procurement
Implementation
EuPRAXIA@SPARC_LAB Machine design
Building design & construction
Final design
Permitting Request
Exec. Design
Validation
Tender for Validation
Tender
Building Construction
Utilities executive design
Tender
Implementation
Acceptance
Building ready
EuPRAXIA@SPARC_LAB Building
Application to prep.phase
Outcome ESFRI application
Preparatory phase
Eupraxia-EU TDR & Legal framework
EuPRAXIA - EU

“Facilities” @LNS and @LNF